CHALMERS

K. ZANDI HANJARI D. CORONELLI

Anchorage Capacity of Corroded Reinforcement

2010:6

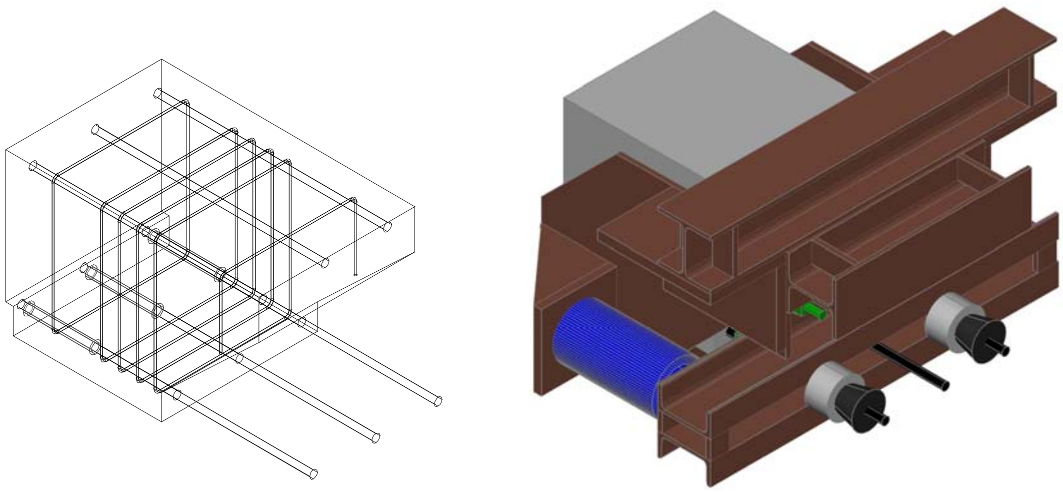

Anchorage Capacity of Corroded Reinforcement

Eccentric Pull-out Tests

K. ZANDI HANJARI

Dept. of Civil and Environmental Eng.
Structural Eng. / Concrete Structures
CHALMERS UNIVERSITY OF TECH
Göteborg, Sweden 2010

D. CORONELLI

Dipartimento di Ingegneria Strutturale
POLITECNICO DI MILANO
Milano, Italy 2010

Report 2010:6

REPORT

Anchorage Capacity of Corroded Reinforcement

Eccentric Pull-out Tests

K. ZANDI HANJARI
Dept. of Civil and Environmental Eng.
Structural Eng. / Concrete Structures
Chalmers University of Technology

D. CORONELLI
Dipartimento di Ingegneria Strutturale
POLITECNICO DI MILANO

Anchorage Capacity of Corroded Reinforcement
Eccentric Pull-out Tests

K. ZANDI HANJARI D. CORONELLI

ISSN 1652-9162
Report

Dept. of Civil and Environmental Eng.
Structural Eng. / Concrete Structures
Chalmers University of Technology
SE-412 96 Göteborg
Sweden
Telephone: + 46 (0)31-772 1000

Dipartimento di Ingegneria Strutturale
POLITECNICO DI MILANO
Piazza L. da Vinci, 32
20133 Milano,
Italy
+39 02 2399.4202

Cover: figures of the test specimen and test set-up, Appendices A and D.

Chalmers reproservice
Göteborg, Sweden 2010

Anchorage Capacity of Corroded Reinforcement
Eccentric Pull-out Tests

K. ZANDI HANJARI
Dept. of Civil and Environmental Eng.
Structural Eng. / Concrete Structures
Chalmers University of Technology

D. CORONELLI
Dipartimento di Ingegneria Strutturale
POLITECNICO DI MILANO

ABSTRACT

There is a growing need for reliable methods of assessing the load-carrying capacity and remaining service life of corroded structures. Previous research has been mainly concerned with lower corrosion levels leading to cover cracking. Moreover, the main focus of the available knowledge concerns the corrosion of the main reinforcement; while the corrosion of the stirrups is often overlooked. Therefore, these two uncertainties ; i.e. high amount of corrosion leading to extensive cover cracking and spalling and the effect of corroding stirrups, were investigated in an experimental program.

Pull-out tests were carried out on eccentrically reinforced specimens with long embedment length to study the anchorage capacity of a corroded bar. The influences of the location of the anchored bar, i.e. middle or corner placement; the presence or absence of transverse reinforcement; the corrosion level of longitudinal reinforcement and the corrosion of transverse reinforcement were studied. The specimens were of three types in relation to the reinforcement arrangement and corrosion: specimens without stirrups, where the main bars were corroded (type A); specimens with stirrups where the main bars were corroded and the stirrups were protected by insulating tape (type B); and specimens with stirrups where the main bars and stirrups were corroded (type C). All of the specimens were subjected to accelerated corrosion, with an average current density of 100 $\mu A/cm^2$, for three time spans that caused a rebar weight loss up to approximately 20% in the main bars and 35% in the stirrups. All of the specimens showed longitudinal cracks along the main bars for relatively low corrosion levels. The corrosion level at first cracking was about 0.6% - 1.0% corrosion weight loss; the cracks widened with increased corrosion levels. Crack patterns formed depended on the presence or absence of stirrups and whether the stirrups were corroded

The crack patterns showed differences between specimens with or without stirrups and when stirrups are corroding or not. The tests showed an important effect of the cover cracking in terms of loss of confinement. They also indicated that the bond behaviour and the failure were strongly governed by the position of the anchored bar, i.e. corner or middle positions, and the level of the corrosion attack. Stirrups played an important role after cover cracking, as they then became the primary source of confinement. The knowledge gained in this study contributes to better understanding of the effects of deterioration on structures.

Contents

ABSTRACT II

CONTENTS 1

PREFACE 3

LIST OF FIGURES 4

LIST OF TABLES 6

1 BACKGROUND AND AIM 8

2 TEST PROGRAM 9

3 TEST ARRANGEMENTS 10

3.1 Choice of the test specimen 10

3.2 Test specimen 11

3.3 Casting and curing of specimens 13

3.4 Accelerated corrosion process 13

3.5 Pull-out test set-up 14

4 MATERIAL PROPERTIES 16

4.1 Concrete 16

4.2 Reinforcement 16

5 ACCELERATED CORROSION TEST RESULTS 19

5.1 Corrosion Level 1 21
5.1.1 Crack width evolution for increasing corrosion 21
5.1.2 Specimens for load test at level 1 26

5.2 Corrosion Level 2 28

5.3 Corrosion Level 3 30

5.4 Crack-corrosion diagrams 34

5.5 Corroded bars 40

6 PULL-OUT TEST RESULTS 47

6.1 Failure mode 47

6.2 Bond strength 47

6.3 Bond versus crack width 51

6.4 Bond stress versus slip 51
6.4.1 Specimens type A: without stirrups 61
6.4.2 Specimens type B: with stirrups 61
6.4.3 Specimens type C: with corroded stirrups 62

7 CONCLUSION 64

8 REFERENCES 65

APPENDIX A TEST SPECIMEN GEOMETRY 67

APPENDIX B ACTUAL CONCRETE COVER 70

APPENDIX C ACTUAL EMBEDMENT LENGTH 71

APPENDIX D TEST SETUP 72

APPENDIX E ARTIFICIAL CORROSION AND CRACK MEASUREMENTS 74

Preface

The tests presented in this report were carried out from June 2008 to December 2010 at the Dipartimento di Ingegneria Strutturale, Politecnico di Milano. The study was initiated throughout a collaboration between Chalmers University of Technology and Politecnico di Milano and it was made possible by the financial support of Politecnico di Milano and the former Swedish Road Administration and Swedish Rail Administration, now both the Swedish Transport Administration.

This report is intended to include details concerning the experimental program and the experimental results. The results of the first and second phases of the program, i.e. artificial corrosion and pull-out test, will be combined with numerical analyses and will be presented in two journal papers, Coronelli *et al.* (2010) and Zandi Hanjari *et al.* (2010b), respectively. More detailed discussion of the test results and numerical analyses will be presented in a doctoral thesis, Zandi Hanjari (2010a).

The authors would like to appreciate all the stimulating discussions with Prof. Gambarova and Marco Lamperti Tornaghi at Politecnico di Milano; Associate Prof. Karin Lundgren, Associate Prof. Mario Plos, Prof. Kent Gylltoft at Chalmers University of Technology; and Jonas Magnusson, Ph.D., at NCC.

Marco Lamperti Tornaghi, at Politecnico di Milano, deserves our greatest gratitude for helping us with technical challenges in the lab. Finally, we would like to extend our thanks to all laboratory staff at Politecnico di Milano.

Kamyab Zandi Hanjari, Göteborg, Sweden

Dario Coronelli, Milano, Italy

List of Figures

Figure 3.1 Schematic illustration of: (a) beam-end region; (b) specimen type A; and (c) specimen types B and C. 10

Figure 3.2 Strut-and-tie model of the test specimen. 11

Figure 3.3 Photo of a fabricated mould for a beam-end specimen. 11

Figure 3.4 Specimen geometry and reinforcement: (a) specimen types A; (b) specimens types B and C; and (c) cross-section of all the three types of specimen. All dimensions are in mm. 12

Figure 3.5 Electorchemical corrosion setup. 13

Figure 3.6 Accelerated corrosion setup. 14

Figure 3.7 Test setup and instrumentation. 15

Figure 4.1 The reinforcement 17

Figure 4.2 Definition of mechanical properties of the reinforcement 18

Figure 4.3 Mechanical properties of steel from a tensile test 18

Figure 5.1 Accelerated corrosion setup. 21

Figure 5.2 Level 1 corrosion crack pattern and crack width-corrosion attack diagrams (Symbols > indicates the location of crack measurement, corresponding to the first crack opening). 22

Figure 5.3 Crack measurements for specimens tested for bond strength at level 1. ... 27

Figure 5.4 Level 2 Crack patterns and width measurements. 29

Figure 5.5 Level 3 crack patterns and width measurements. 32

Figure 5.6 Crack-corrosion diagrams and synthesis of results (opening, level 1, 2 and 3). 35

Figure 5.7 Gravimetric measurements for repeated cycles (ISO 8407). 42

Figure 5.8 The corrosion attack of the main bars from the bottom. 43

Figure 5.9 Type B specimens: uncorroded stirrup surface, after removing the protection tape. 43

Figure 5.10 Stirrup corrosion in specimen C3c: (a, c, d) Partial breaking of the cover due to the load test on the specimen; (b) cover removed by hammering and pneumatic drilling; (e-f) corroded stirrups exposed by drilling the surrounding concrete. 44

Figure 5.11 Morphology of the corroded bar surface. 45

Figure 6.1 Crack patterns at different failure modes observed in tests. 47

Figure 6.2 Overview of the test results in terms of bond strength normalized with respect to that of the middle bar in reference specimens, versus corrosion attack. 49

Figure 6.3 Overview of the test results in terms of bond strength normalized with respect to that of the middle bar in reference specimens, versus total crack width. ... 51

Figure 6.4 Average bond stress versus free-end slip measured in the pull-out tests for specimens B1c and the reference specimens. 52

Figure 6.5 Average bond stress versus free-end slip measured in the pull-out tests for specimens B1m2 and the reference specimens. 53

Figure 6.6 Average bond stress versus free-end slip measured in the pull-out tests for specimens A2c and the reference specimens. 54

Figure 6.7 Average bond stress versus free-end slip measured in the pull-out tests for specimens A2m and the reference specimens. 55

Figure 6.8 Average bond stress versus free-end slip measured in the pull-out tests for specimens B2m1 and the reference specimens. 56

Figure 6.9 Average bond stress versus free-end slip measured in the pull-out tests for specimens C2m2 and the reference specimens. 57

Figure 6.10 Average bond stress versus free-end slip measured in the pull-out tests for specimens B3m1 and the reference specimens. 58

Figure 6.11 Average bond stress versus free-end slip measured in the pull-out tests for specimens B3m2 and the reference specimens. 59

Figure 6.12 Average bond stress versus free-end slip measured in the pull-out tests for specimens C3c and the reference specimens. 60

Figure 6.13 Crack pattern after pull-out test of corner bars in tow reference specimens of type B. 62

List of Tables

Table 2.1 Test program. *9*

Table 4.1 Concrete mix compositions. *16*

Table 4.2 Results from compressive strength tests on 150 mm cube. *16*

Table 4.3 Mechanical properties of the reinforcement *17*

Table 5.1 Test program *19*

Table 5.2 Maximum corrosion levels *20*

Table 5.3 Specimens for load test at Level 1 .... *26*

Table 5.4 Specimens for load test at Level 2 .... *28*

Table 5.5 Specimens for load test at Level 3. .... *31*

Table 5.6 Corrosion attack, results of gravimetric measurements. *41*

Table 5.7 Corrosion levels - Stirrups *42*

Table 6.1 Average bond strength, results from pull-out tests. *50*

1 Background and aim

Corrosion of steel reinforcement is one of the most common causes of deterioration of reinforced concrete. Some existing concrete structures like parking garages, harbours and bridges show significant corrosion; it is not uncommon that cover spalling has occurred. An important question is how reliable these structures are; how the load-carrying capacity of corrosion-damaged structures can be calculated? Previous research, fib (2000), has been mainly concerned with corrosion levels leading to cover cracking; while relatively little attention has been devoted to higher levels of corrosion causing cover delamination. This is a practically important problem, both for assessment of the residual load-carrying capacity of corrosion-damaged concrete structures, but also for lifetime design of new structures. Moreover, the main focus of the available knowledge concerns with the corrosion of the main reinforcement; while the corrosion of the stirrups is often overlooked. Field investigations have showed that cover delamination is more probable in areas of tightly spaced stirrups. A rather common approach in modelling the effect of the corroded stirrups is to consider the loss of the cross-sectional area. However, if the effect of corroded stirrups on crack initiation, crack propagation and cover delamination is not considered, this will lead to overestimation of the load-carrying capacity of the corroded structure.

When studying the anchorage of a ribbed bar in structural concrete members, the anchorage capacity is strongly influenced by the actual confinement conditions. In general, confinement is a result of the surrounding concrete, stirrups and transverse pressure fib (2000). The corrosion of reinforcement leads to volume expansion of the steel, which generates splitting stresses in the concrete influencing the bond between concrete and reinforcement. For a larger corrosion penetration, the splitting stresses may lead to cover cracking and, finally, spalling of the concrete cover. In the extreme case, when cover spalling occurs, the resisting mechanism in the cross section is altered and stirrups become the main source of confinement.

Accelerated corrosion tests are widely used in laboratories to study the mechanical properties of deteriorated RC specimens. The chemo-physical effects are different from those of natural corrosion Yuan *et al.* (2007). From the mechanical point of view, some concerns exist regarding spurious bond deterioration obtained with high current densities. This study assumes that a sufficiently slow accelerated corrosion test can produce cross-section loss, concrete cracking and bond deterioration approximating natural corrosion, as far as the mechanical effects on RC structures are concerned.

This experimental program contributes to the understanding of the anchorage behaviour of severely corroded bars. The combined effects of high corrosion penetrations and of corroding stirrups on the anchorage regions are investigated.

2 Test program

Eccentric pull-out tests were carried out to investigate the anchorage capacity of a severely corroded bar. The location of the bar, middle or corner position, the amount of transverse reinforcement, and the corrosion level of longitudinal and transverse reinforcement were included in the study. The test program is summarised in Table 2.1. Since a high scatter of results is usually expected in this type of test, 18 specimens were cast. Half of the total number of specimens was made without sodium chloride, while the rest were cast with 3% sodium chloride mixed into concrete to accelerate the corrosion process.

The specimens were of three types with respect to the reinforcement arrangement and corrosion of main bars and stirrups:

- Type A: without stirrups, main bars were subjected to corrosion,
- Type B: with stirrups, only main bars were subjected to corrosion, and
- Type C: with stirrups, main bars and stirrups were subjected to corrosion.

Note: the specimens were preliminary named after casting, which was marked on each specimen (this name appears on the photos of specimens). After the specimens were artificially corroded, they were renamed. This final name is used in this report and is given in the caption of each photo.

Pull-out tests were carried out on reference specimens and corroded specimens at three levels:

- Level 1 corresponded to cracks occurring along the main reinforcement; at a corrosion level lower than 2% weight loss in the main bars;
- Level 2 corresponded to a corrosion level of 2-10% weight loss in the main bars; and
- Level 3 corresponded to extensive cover cracking, at a corrosion level greater than 10% weight loss in the main bars.

Table 2.1 Test program.

Corrosion level	Weight loss of main bars [%]	Corrosion cracking [mm]	Position of tested bar(s)	n° of specimens		
				Type A	Type B	Type C
Reference	No corrosion	No cracks	Middle bar	3	2	–
			Corner bars	2	2	–
Level 1	~ 0-2	< 0.4	Middle bar	–	1	–
			Corner bars	–	1	–
Level 2	~ 2-10	0.4-1.0	Middle bar	1	–	–
			Corner bars	1	1	
Level 3	~ 10-20	> 1	Middle bar	–	1	1
			Corner bars	–	1	1

3 Test arrangements

3.1 Choice of the test specimen

The geometry of the eccentric pull-out specimens was similar to that used by Magnusson (2000), which had the shape of a beam-end after inclined shear cracking; see ***Figure 3.1***. The behaviour of the eccentric pull-out test shares some similarities and dissimilarities with a beam-end region. For example, similar to a beam-end region, the inclined strut is carried both on the anchored bar and the support region. However, in the test specimens, the main bars were not in contact with the concrete over the support. The effect of support pressure and the anchorage of the bar over the support are therefore not the same as it is at the end of a beam.

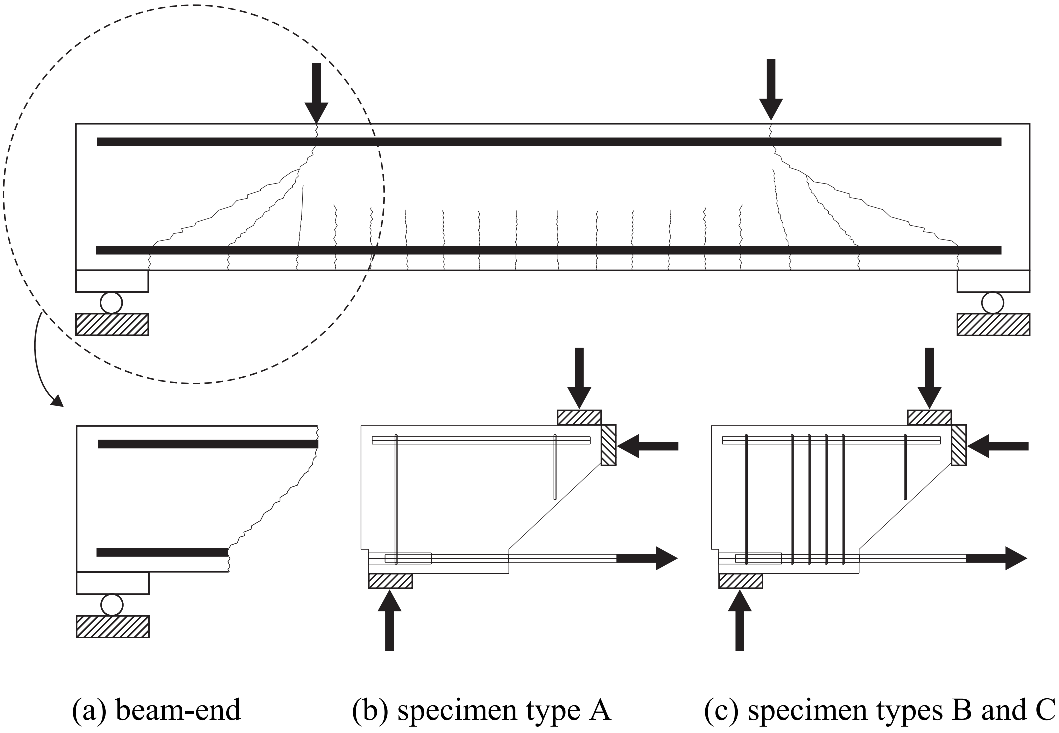

Figure 3.1 Schematic illustration of: (a) beam-end region; (b) specimen type A; and (c) specimen types B and C.

The strut-and-tie model of the test specimen is shown in ***Figure 3.2***. There was a risk for a shear crack to take place starting from the end of the free-zone towards the support at the top. Therefore, to avoid shear failure of the test specimens, two stirrups were placed outside the embedment length, one at the support and the other in the “nose”. This was done in all specimen types.

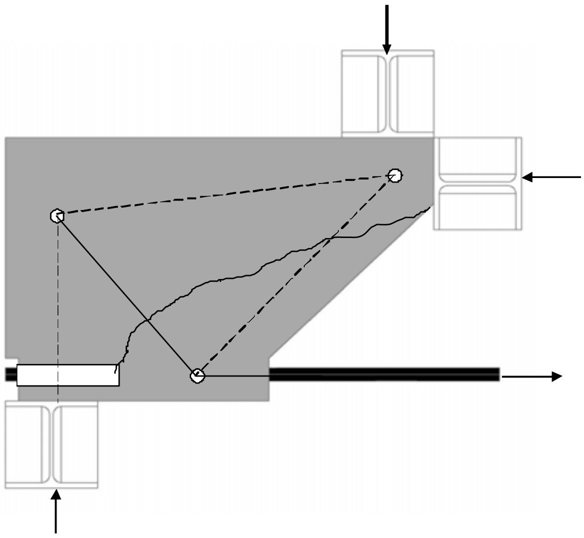

Figure 3.2 Strut-and-tie model of the test specimen.

3.2 Test specimen

In total eighteen wooden moulds were made for the test specimens, see Figure 3.3. Two different reinforcement arrangement, with and without transverse reinforcement along the embedment length, were fabricated; the geometry of the specimens are given in Figure 3.4. The specimens were cast with the main longitudinal reinforcement of 20 mm in the horizontal position at the bottom of the moulds, and with a transverse reinforcement of 8 mm. A small concrete cover to the main bar, 1.5 times the main bar diameter, was used. The main bars were in contact with the concrete over a 210 mm embedment length; the bond-free zone over the support, 190 mm, reduced the direct effect of support pressure. As mentioned before, the areas outside the embedment length, the bond-free zone and the "nose", were reinforced by transverse reinforcement to avoid any unfavourable failure mode.

The reinforcing bars which were not supposed to be corroded, such as the reinforcement in compression zone and stirrups in some of the specimens, were taped using PVC electrical insulation tape. The main longitudinal reinforcements were covered by silicon glue along the bond-free zone. The specimen geometry and reinforcement detailing are shown in Appendix A.

Figure 3.3. Photo of a fabricated mould for a beam-end specimen.

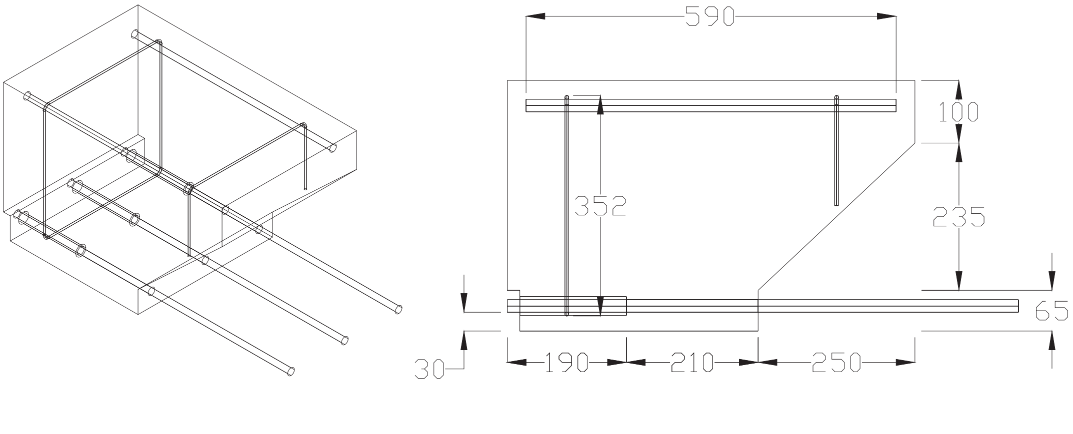

(a)

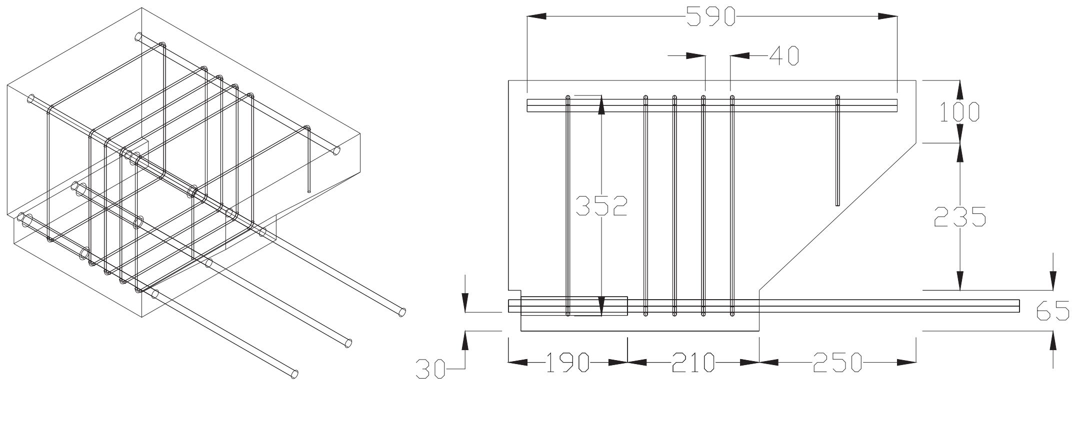

(b)

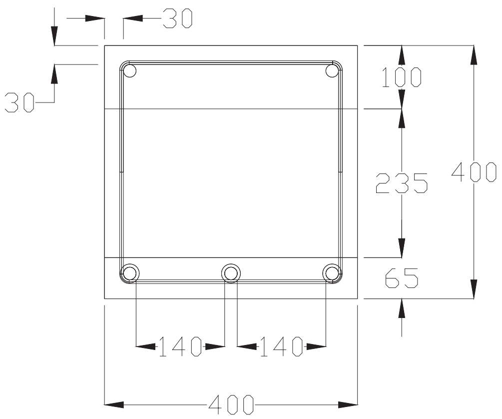

(c)

Figure 3.4. Specimen geometry and reinforcement: (a) specimen types A; (b) specimens types B and C; and (c) cross-section of all the three types of specimen. All dimensions are in mm.

3.3 Casting and curing of specimens

Before casting, the reinforcing bars were wire-brushed to remove any scale and weighted to a precision of two decimal places. The specimens were cast with the main longitudinal reinforcement in the horizontal position at the bottom of the moulds. The specimens were kept in a laboratory environment until 28 days after which they were demoulded and kept in a curing room at 20˚C and 50% RH.

3.4 Accelerated corrosion process

Specimens were corroded by an electrochemical method using impressed current. During the corrosion process, the specimens were placed upside down, with the main bars near the top; see

Figure ***3.5***. The current flowed through the main bars across the top concrete cover to a cathode placed at the top of the beam, inside a tank containing a solution of 3% chloride. Thus, the corrosion attack took place from one direction. All the specimens were connected to a generator in a series circuit, see Figure 3.6. Stirrups in the type B specimens were insulated using PVC electrical tape to prevent corrosion. The current density was low with an average value of 100 μA/cm^2. Specimens were corroded up to 10 months, reaching approximately 2% weight loss for each month. When compared with artificial corrosion tests in the literature, this can be considered a low value. Other researchers have used faster rates, by as much as one order of magnitude. Spurious mechanical concrete-steel bond deterioration has been measured for high current density values, see Saifullah and Clark (1994) and Yuan *et al.* (2007); for a review of the effect of corrosion rate on bond strength, see Sæther (2009) and Sæther *et al.* (2007). Pull-out tests were carried out on reference specimens and corroded specimens at three levels, see also Table 1:

- Level 1 corresponded to cracks occurring along the main reinforcement; at a corrosion level lower than 2% weight loss in the main bars;
- Level 2 corresponded to a corrosion level of 2-10% weight loss in the main bars; and
- Level 3 corresponded to extensive cover cracking, at a corrosion level greater than 10% weight loss in the main bars.
-

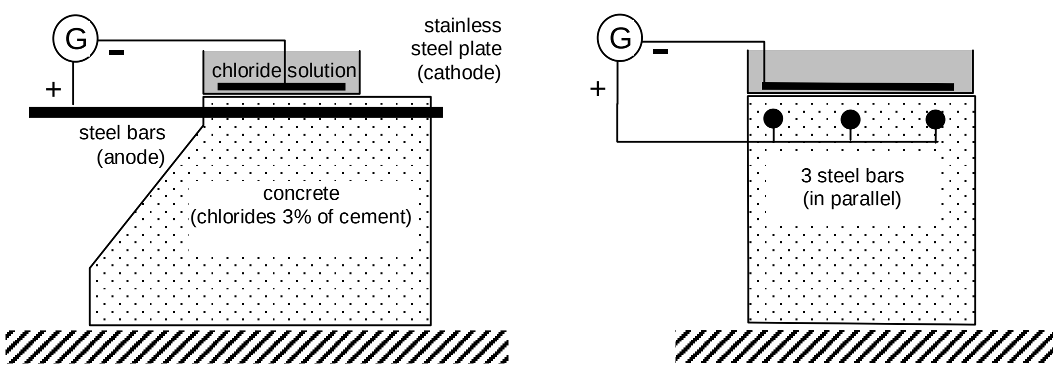

Figure 3.5 Electorchemical corrosion setup.

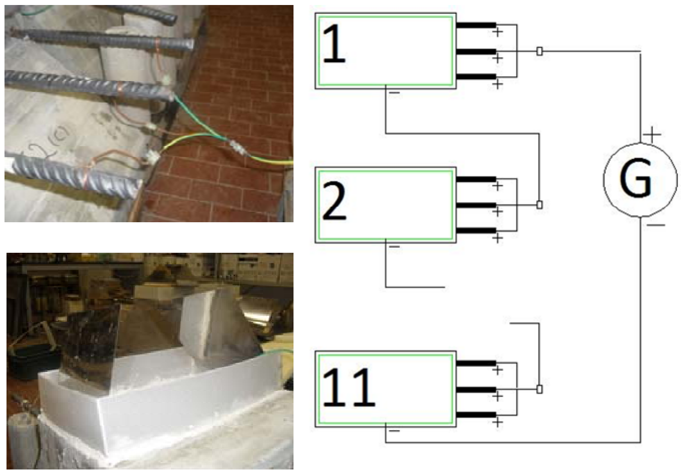

Figure 3.6 Accelerated corrosion setup.

Corrosion attack was determined theoretically using Faraday's law and *a posteriori* by weight loss measurements. This was done for all specimens except one which was kept for another phase of the research program. The average difference between the two methods was approximately 10%; the corrosion penetrations were overestimated by Faraday's law. Crack widths on the bottom and side covers were measured during the corrosion process using a microscope with a resolution of 0.04 mm up to corrosion level 1. Beyond that level of corrosion, most cracks were filled by corrosion products to a point that the optic device could no longer be used. Crack widths at levels 2 and 3 were measured before the load testing using a reference ruler with a range of graded lines, each corresponding to a specified width.

3.5 Pull-out test set-up

The specimens were tested in a specially designed test rig. The test set-up is outlined in Figure 3.7; more detailed drawings are given in Appendix D. Deformation control was adopted to permit measurements of the post-peak behaviour. The loading was controlled by displacement, with the active end of the main bar being pulled out. The deformation rate was initially about 0.10 mm/minute; after the maximum load capacity was reached, the deformation rate was increased in steps to a maximum rate of about 0.50 mm/minute. In each test either the middle bar or the two corner bars of the specimen were pulled out.

The tensile force in the bars was measured using load cells. Instrumentation was provided to measure the relative displacement of the main bars at both the active and passive ends relative to the stable faces of the specimen. When the corner bars were tested, the two bars were loaded simultaneously. Displacement was controlled using two LVDTs, and the loads were read using two load cells mounted on each individual bar; it was, therefore, possible to register the individual response of each bar.

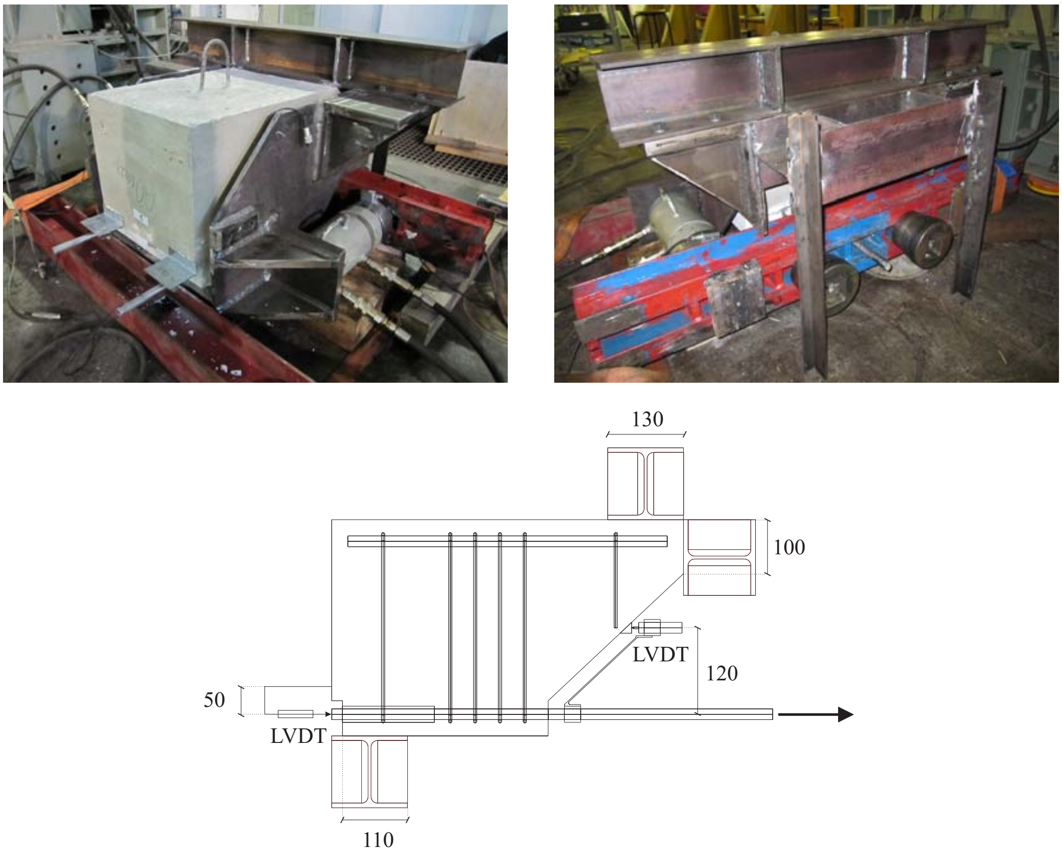

Figure 3.7 Test setup and instrumentation.

4 Material properties

4.1 Concrete

Test specimens were cast with a concrete of grade C30/37 mixed in two batches: Mix I with 3% sodium chloride and Mix II without sodium chloride; see Table 4.1. The compressive and tensile strengths of the concrete were measured using 150 mm cube cast from the same concrete batches. All of the specimens were kept in a laboratory environment for 28 days, after which they were demoulded and kept in a curing room at 20˚C and 50 % relative humidity. The concrete compressive strength is presented in Table 4.2.

Table 4.1 Concrete mix compositions.

Constituents	Mix I: without NaCl		Mix II: with 3% NaCl	
	Density [kg/m^3]	**Mix [kg/m^3]**	**Density [kg/m^3]**	**Mix [kg/m^3]**
Cement	3100	360	3100	360
Water	1000	205	1000	205
Aggregate: sand 0-4 mm	2530	990.1	2530	990.1
Aggregate: Gravel 5-10 mm	2630	777.9	2630	777.9
3 % Sodium chloride (NaCl)	-	-	216.5	10.8
Water/cement ratio		0.57		0.57

Table 4.2 Results from compressive strength tests on 150 mm cube.

Concrete age	Specimen type	Mix type	Compressive Strength [MPa]	Average [MPa]	Cov [%]
28 days	Cube	I	37	38	4.7
	Cube	I	38		
	Cube	I	41		
	Cube	I	36		
	Cube	I	37		
	Cube	I	39		
	Cube	II	35	34.3	1.7
	Cube	II	34		
	Cube	II	34		

4.2 Reinforcement

The deformed hot-rolled bars used in the specimens were of Ø20 for the longitiudianl reinforcement (in compression and tension side) and of Ø8 for the stirrups; see Figure 4.1. The material properties of the reinforcement are given in Table 4.3 and Figure

4.2. The tensile tests on bars Ø20 were carried out according to a standard procedure at the laboratory of Structural Engineering at Politecnico di Milano; see Table 4.3.

(a) Rebar Ø20 (b) Rebar of Ø20

Figure 4.1 The reinforcement

Table 4.3 Mechanical properties of the reinforcement

Specimen	A_s **[mm²]**	f_{sy} **[MPa]**	f_{su} **[MPa]**	ε_{sy} **[%]**	ε_{s2} **[%]**	ε_{su} **[%]**
1	314.16	505.94	616.78	13.09	20.31	64.93
2	314.16	511.33	620.13	21.06	28.36	77.83
3	314.16	509.90	620.01	18.64	26.32	80.89
4	314.16	509.42	617.98	18.75	26.05	79.61
5	314.16	512.05	622.65	18.96	26.20	77.19
Average	314.16	509.73	619.51	18.10	25.45	76.09

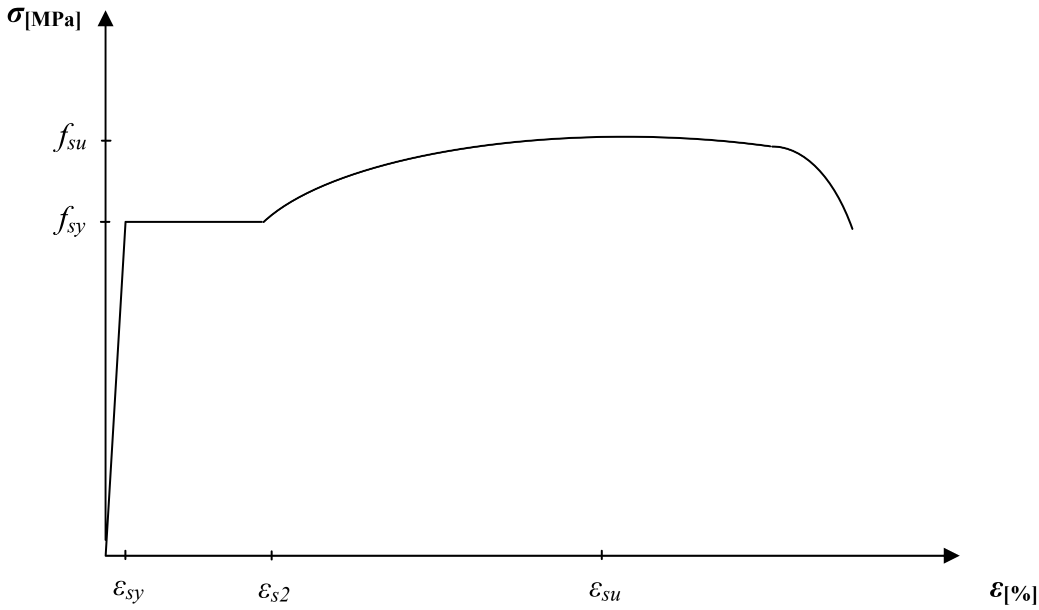

Figure 4.2 Definition of mechanical properties of the reinforcement

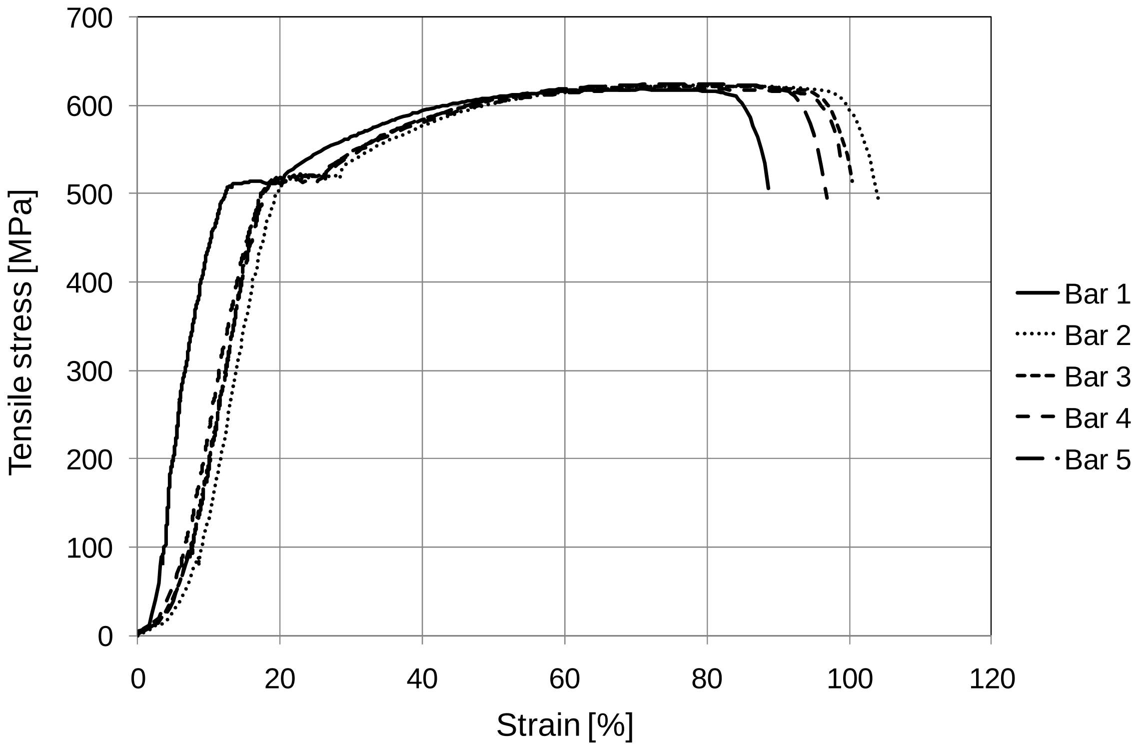

Figure 4.3 Mechanical properties of steel from a tensile test

5 Accelerated corrosion test results

During the corrosion phase the corrosion attack values were determined theoretically using Faraday's law. The maximum level reached for each bar was also measured *a posteriori* by weight loss measurement. The difference between the two on average was approximately 10%.

The main reinforcement bars were extracted from the concrete after the load testing, breaking up the specimens. The maximum corrosion levels were measured by weight loss measurements with the method of the ISO 8407 standard. The results for all corroded bars are given in Tables 5.2 and 5.6.

The corrosion level for one Type B and two Type C specimens was calculated only from the circulated current, because these specimens will be subjected to mechanical testing later and thus have not yet been broken up.

Crack widths on the bottom cover (in the corrosion setup the top surface of the specimen, see Figure 5.1) were measured during the corrosion process using a microscope with a resolution of 0.04mm up to corrosion Level 1.

Beyond this level, most cracks were filled by corrosion products to a point that the optic device could no longer be used. Crack widths at Levels 2 and 3 were measured before the load testing using a reference ruler with a range of graded lines, each corresponding to a specified width.

Table 5.1 Test program

Specimens and corrosion levels	Position of bar(s) tested for bond strength.	Number of specimens		
		Without stirrups (1) (Type A)	With non-corroded stirrups (1) (Type B)	With corroded stirrups (1) (Type C)
Reference - 0% corrosion	Middle bar	3	3	×
	Corner bars	2	3	×
Level 1 - Cracks along the main reinforcement; 1-2% corrosion	Middle bar	×	1	×
	Corner bars	×	1	×
Level 2 - Propagation of cracks; approximately 10% corrosion	Middle bar	1	×	×
	Corner bars	1	2	1
Level 3 - High Corrosion (approximately 15% corrosion)	Middle bar	×	2	1
	Corner bars	×	1	1

(1) Along the embedment length

Table 5.2 Maximum corrosion levels

Level	Specimen	Rebar no	Corrosion (%)	average attack (micron)	position (°)
1	**B1c**	31	3.5	176	left
	B1c	28	1.4	72	central
	B1c	3	0.2	10	right
	B1m2	22	0.2	11	left
	B1m2	48	0.7	36	central
	B1m2	29	2.1	104	right
2	**A2c**	25	7.3	372	left
	A2c	13	8.5	434	central
	A2c	35	8.9	456	right
	A2m	12	7.2	369	left
	A2m	16	4.5	228	central
	A2m	34	9.0	459	right
	B2m1	42	12.4	641	left
	B2m1	32	4.2	210	central
	B2m1	33	7.7	394	right
	C2m2	2	9,8 (*)	500	left
	C2m2	15	7,0 (*)	350	central
	C2m2	36	15,5 (*)	810	right
3	**B3c**	17	10,9 (*)	560	left
	B3c	38	11,6 (*)	590	central
	B3c	43	12,9 (*)	660	right
	B3m1	23	13.0	671	left
	B3m1	21	14.8	768	central
	B3m1	20	13.5	699	right
	B3m2	19	15.7	820	left
	B3m2	41	14.0	724	central
	B3m2	40	9.2	473	right
	C3c	38	7.0	359	left
	C3c	37	16.7	872	central
	C3c	15	11.1	570	right
	C3m1	45	20,7 (*)	1100	left
	C3m1	24	19,1 (*)	1010	central
	C3m1	44	21,0 (*)	1110	right

(^) Mark: Specimen type (A, B, C) – Final Corrosion level (1, 2, 3) – Bar to be loaded in bond tests (c = corner; m = middle) – Specimen nr. (1, 2).

(*) Calculated from the circulated current.

(°) Front view with bars on the top (corrosion setup).

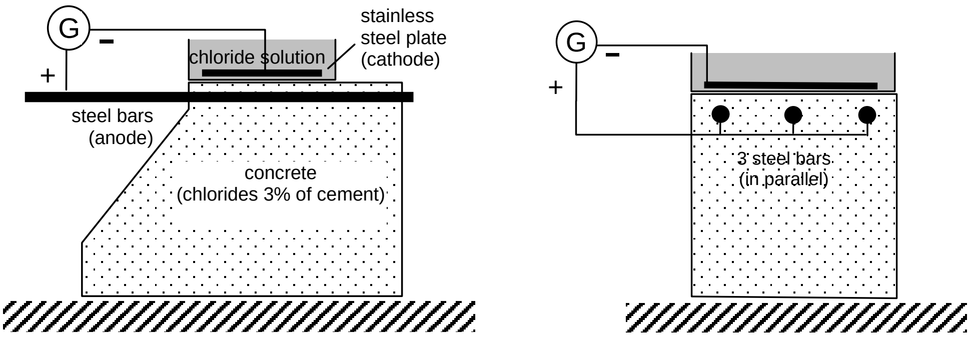

setup)

Figure 5.1 Accelerated corrosion setup.

5.1 Corrosion Level 1

5.1.1 Crack width evolution for increasing corrosion

Between corrosion initiation and level 1 all specimens showed longitudinal cracks along the main bars. The cover around each bar is cracked radially; either the side or bottom or both covers were cracked. The first corrosion cracks opened around 30-50 microns attack, on the bottom cover (top cover during corrosion); for these measurements at intervals were made using a microscope. The corresponding corrosion was calculated from the circulated current (see Appendix E). The diagrams obtained are shown in Figure 5.2, together with the crack patterns. The test results are compared to the predictions of the model by Vidal *et al.* (2004).

A) Specimens without stirrups

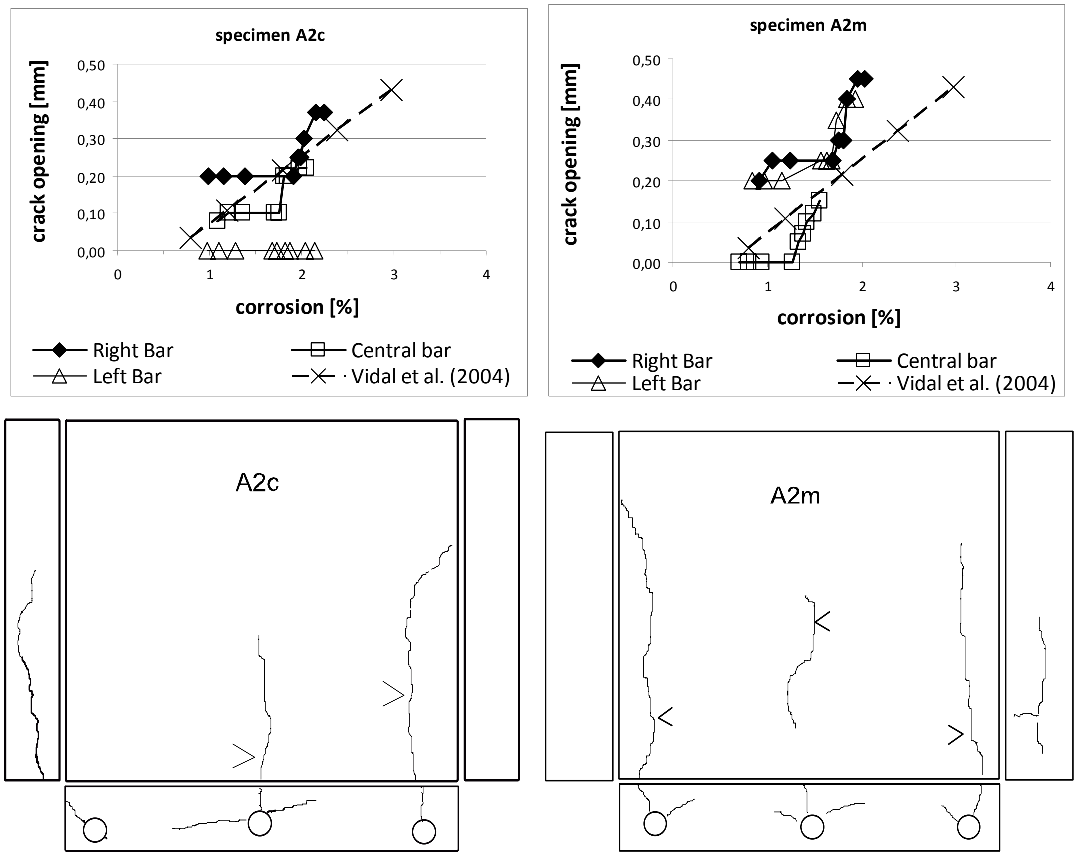

Figure 5.2 Level 1 corrosion crack pattern and crack width-corrosion attack diagrams (Symbols > indicates the location of crack measurement, corresponding to the first crack opening).

B) Specimens with stirrups

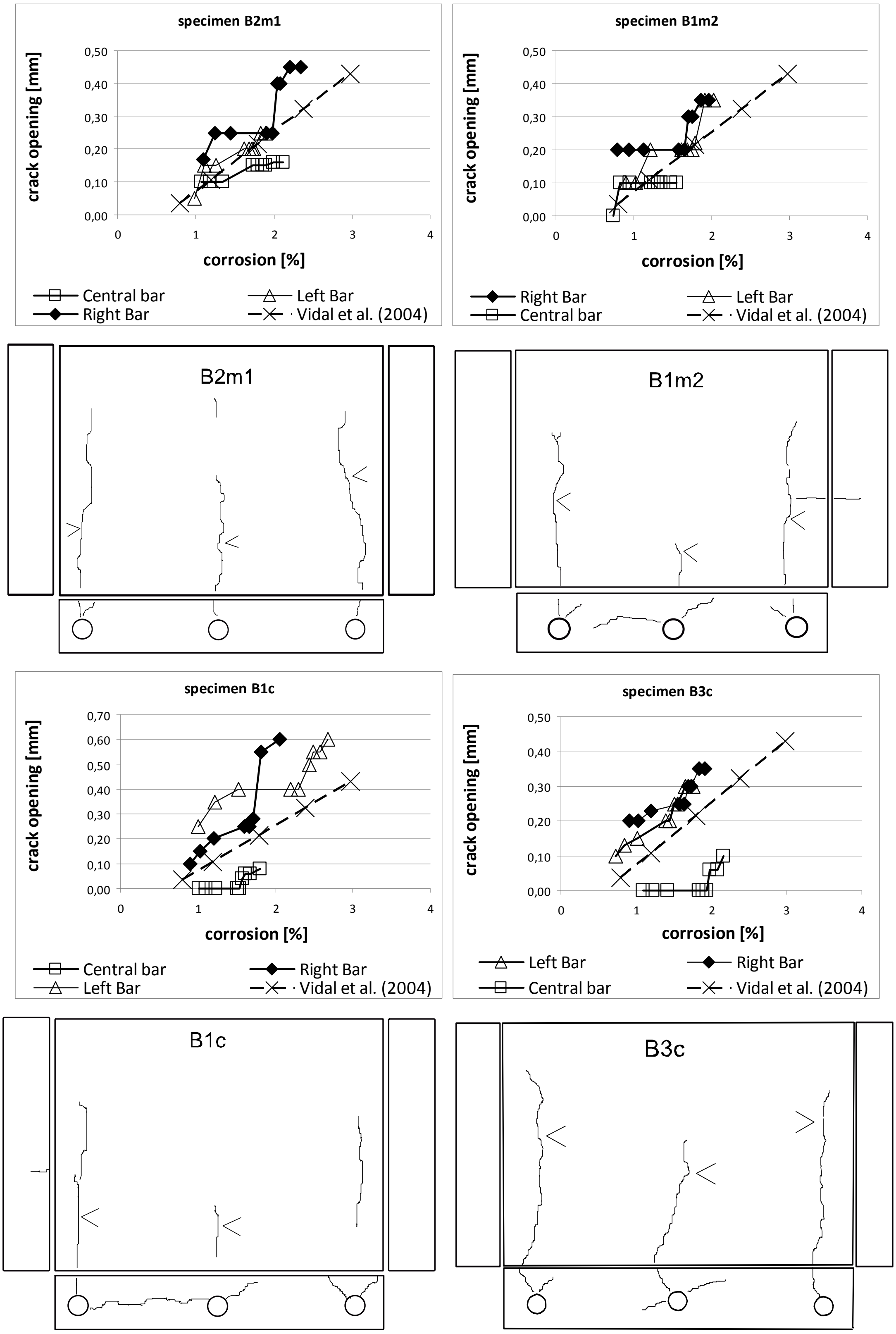

Figure 5.2 (Continued): Level 1 corrosion crack pattern and crack width-corrosion attack diagrams (Symbols > indicates the location of crack measurement, corresponding to the first crack opening).

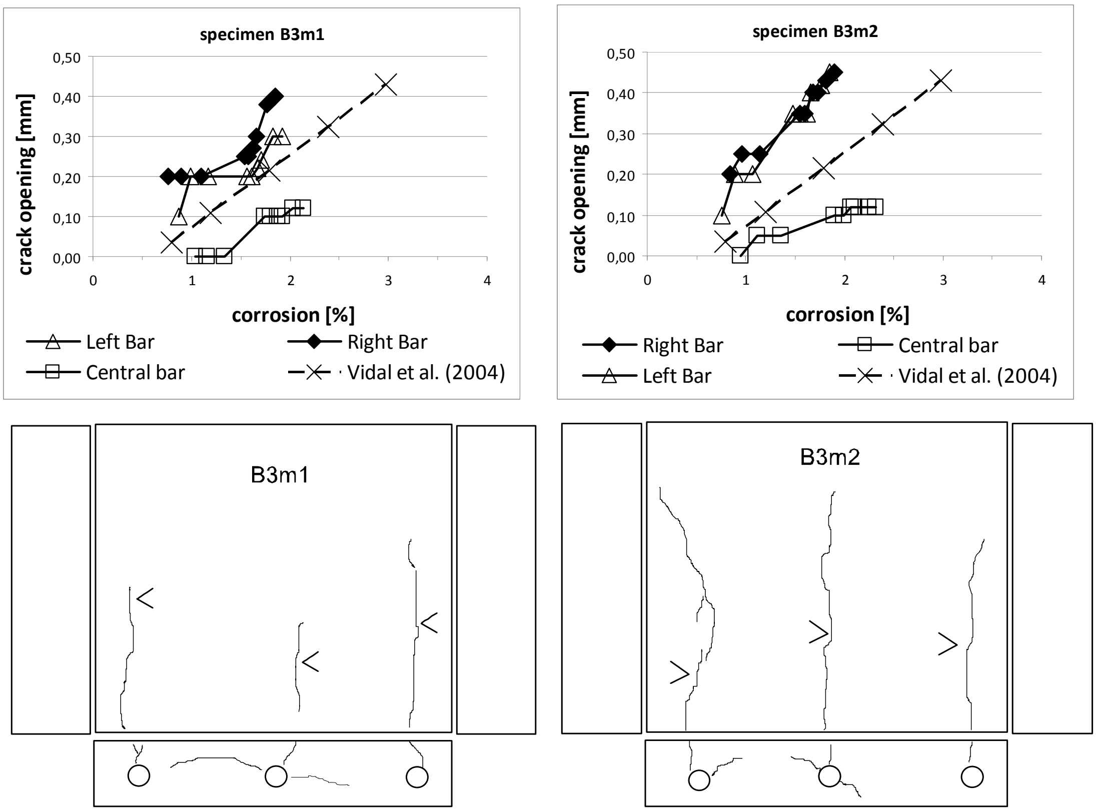

Figure 5.2 (Continued): Level 1 corrosion crack pattern and crack width-corrosion attack diagrams (Symbols > indicates the location of crack measurement, corresponding to the first crack opening).

C) Specimens with corroding stirrups

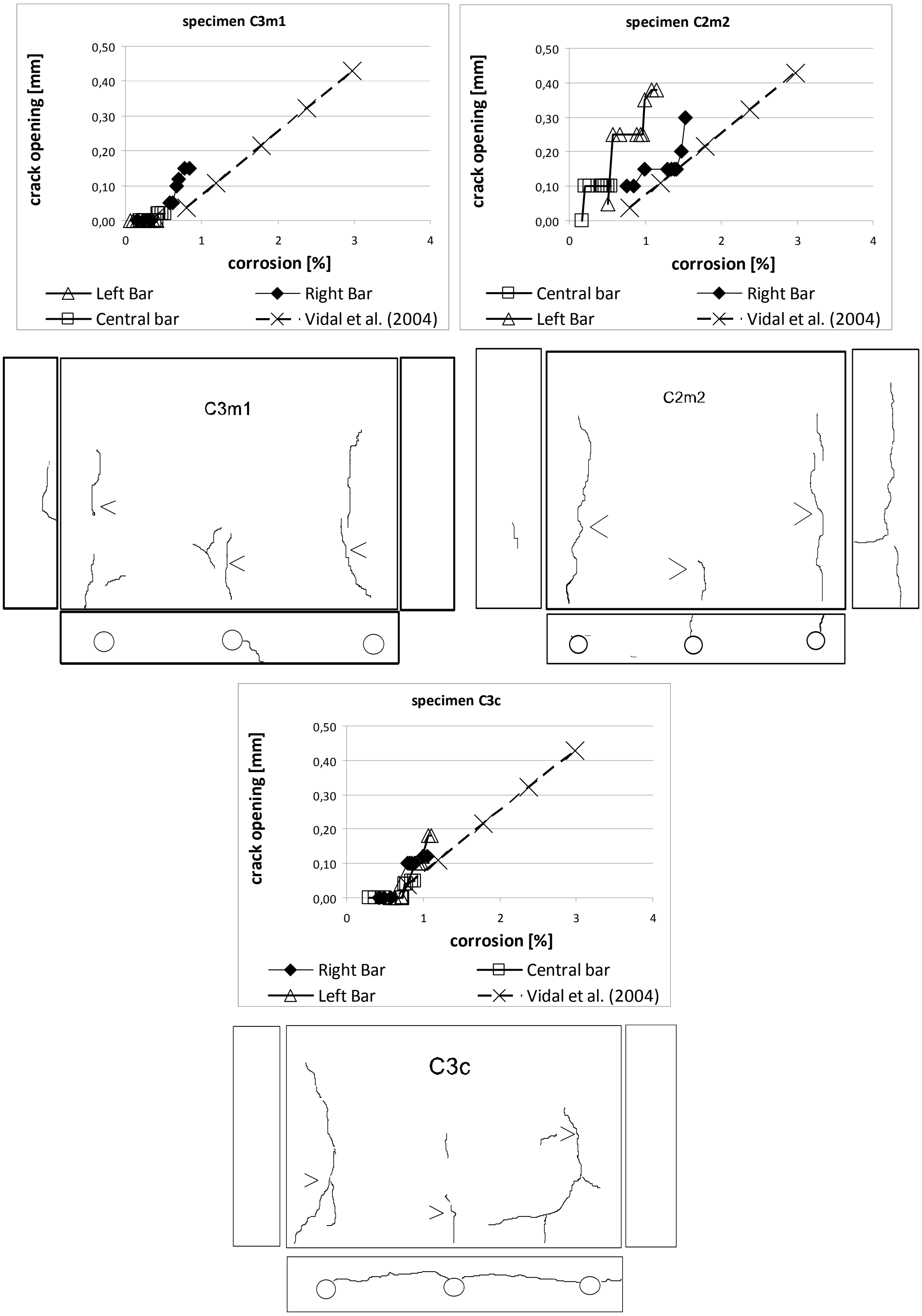

Figure 5.2 (Continued): Level 1 corrosion crack pattern and crack width-corrosion attack diagrams (Symbols > indicates the location of crack measurement, corresponding to the first crack opening).

5.1.2 Specimens for load test at level 1

Two specimens were tested for bond in correspondence of Level 1 corrosion. The crack patterns and width values are shown in Figure 5.3. The corrosion was stopped on 2009.02.14 and load tests carried out on 2009.04.15. All cracks were measured before the load test. Some crack values are higher than those shown in the graphs in the previous section, because of some ongoing corrosion in these two months.

Table 5.3 Specimens for load test at Level 1

Level	Specimen (^)	weight loss (%)	average attack (mm)	position (°)
1	B1(c)	3.5	176	left
		1.4	72	central
		0.2	10	right
	B1(m2)	0.2	11	left
		0.7	36	central
		2.1	104	right

(*) Corrosion calculated using Faraday's law.
(°) Front view with bars on the top (corrosion setup).
Note: see Section 5.5 for corrosion attack measurements

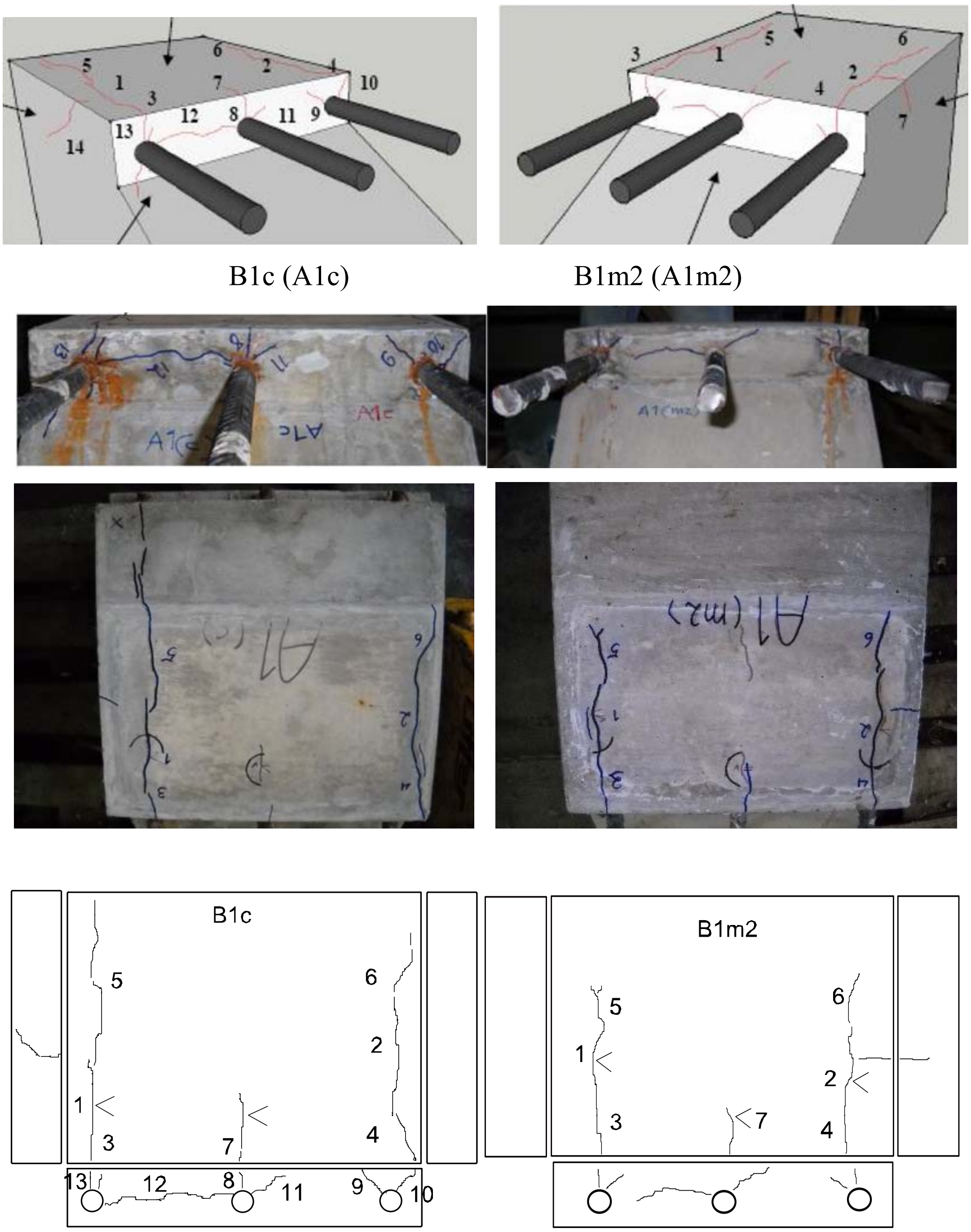

Specimen B1c

Crack nr.	1	2	3	4	5	6	7	8	9	10
Width (mm)	0.8	0.8	0.6	0.7	0.55	0.9	0.1	0.1	0.1	0.1
Crack nr.	11	12	13	14						
Width (mm)	0.06	0.1	0.1	0.2						

Specimen B1m2

Crack nr.	1	2	3	4	5	6	7
Width (mm)	0.4	0.4	0.4	0.3	0.1	0.5	0.1

Figure 5.3 Crack measurements for specimens tested for bond strength at level 1.

5.2 Corrosion Level 2

The measurements of the bottom cover cracks were suspended because the accumulation of corrosion products made these observations not accurate; only final crack widths before the load testing were measured for the specimens listed in Table 5.4. The crack patterns and the final crack width values are shown in Figure 5.4. Some general comments on the evolution of cracking in the three different groups of specimens are given in the following.

Table 5.4 Specimens for load test at Level 2

Level	Specimen (^)	weight loss (%)	average attack (mm)	position (°)
2	A2(c)	7.3	372	left
		8.5	434	central
		8.9	456	right
	A2(m)	7.2	369	left
		4.5	228	central
		9.0	459	right
	B2(m1)	12.4	641	left
		4.2	210	central
		7.7	394	right
	C2(m2)	9,8 (*)	500	left
		7,0 (*)	350	central
		15,5 (*)	810	right

(*) Corrosion calculated using Faraday's law.
(°) Front view with bars on the top (corrosion setup).
Note: see Section 5.5 for corrosion attack measurements

Specimens without stirrups (Type A)

The cracks run mainly along the longitudinal reinforcement. These specimens showed fewer and wider cracks than those with stirrups. In one of the specimens a delamination plane formed connecting two bars, with a maximum crack width of 1.4 mm.

Specimens with non corroded stirrups (Type B)

Longitudinal cracks showed in bottom and side covers. The crack pattern on the front cover is:

- cracks radiating from the bar to the closest point of the outer surface;
- cracks lying in a horizontal plane;
- cracks in inclined planes forming a "V-shaped" pattern.

On the side covers, longitudinal and transverse cracks form.

Specimens with corroded stirrups (Type C)

Specimens C showed two different crack patterns:

- bottom cover cracking, with corrosion products showing in big stains on the outer surface; many small cracks open, both longitudinally and in other directions (not shown in the drawings);

- initiation of delamination cracks, forming a plane across the bars, and front and side cover cracking.

On the whole the presence of stirrups causes a more complex crack pattern than for specimens without stirrups, both when these are non corroding or corroding.

A) Specimens without stirrups

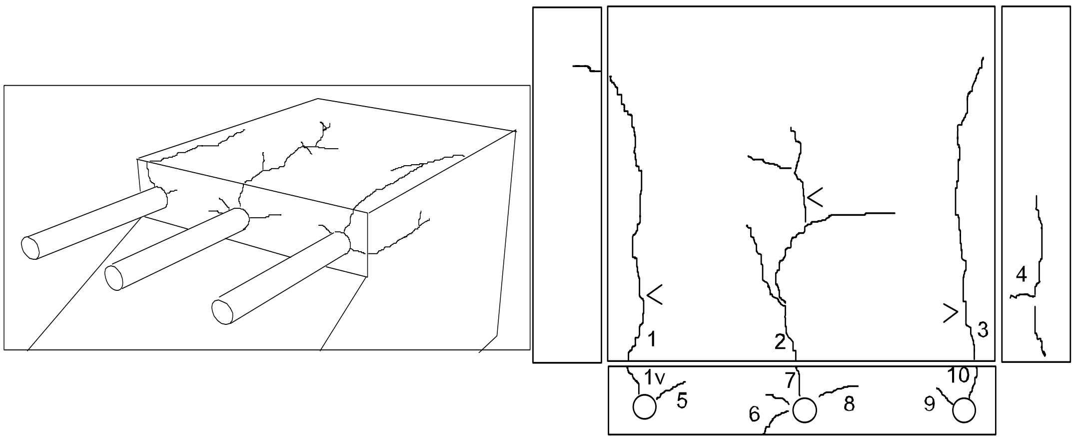

Specimen A2m

Crack nr.	1	1v	2	3	4	5	6	7	8	9	10
Width (mm)	0.8	0.7	0.3	0.5	0.3	0.3	0.2	0.3	0.2	0.2	0.3

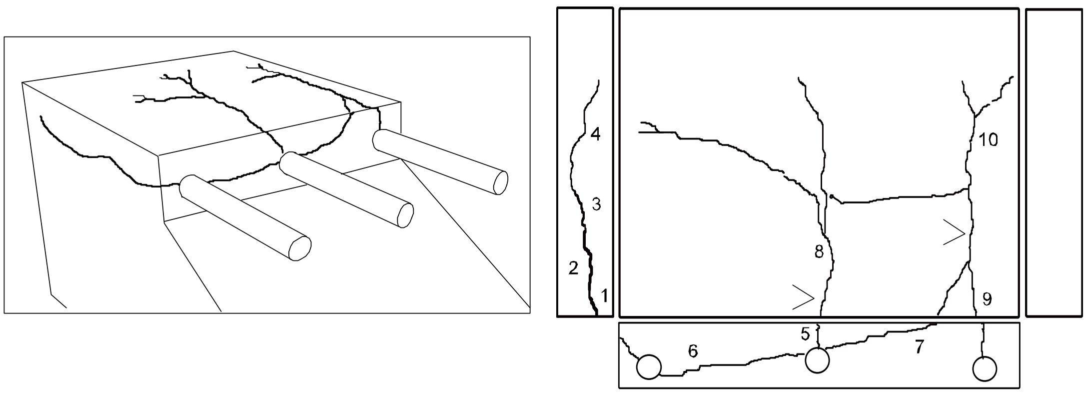

Specimen A2c

Crack nr.	1	2	3	4	5	6	7	8	9	10
Width (mm)	1,4	1	1	0,9	0,5	0,5	0,2	0,4	0,6	0,4

Figure 5.4 Level 2 Crack patterns and width measurements.

B) Specimens with non-corroding stirrups

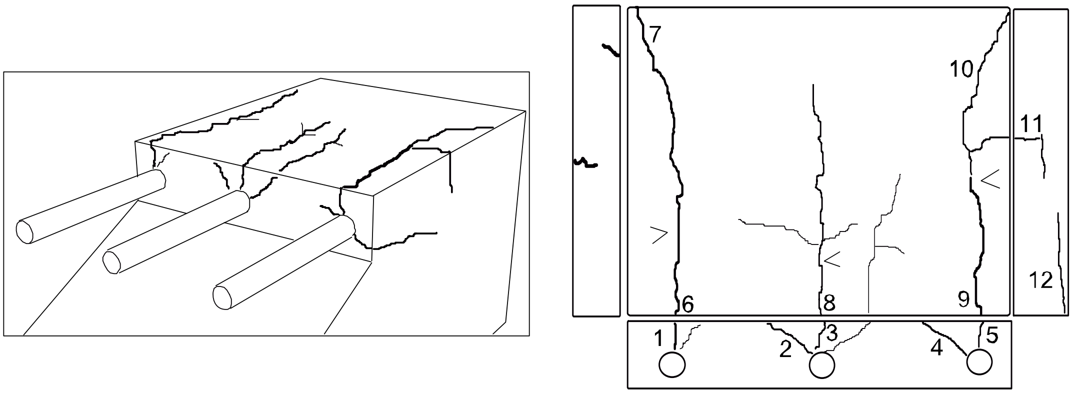

Specimen B2m1

Crack nr.	1	2	3	4	5	6	7	8	9	10	11	12
Width (mm)	0,5	0,3	0,35	0,2	0,4	0,5	0,9	0,4	0,4	0,3	0,4	0.2

C) Specimens with corroding stirrups

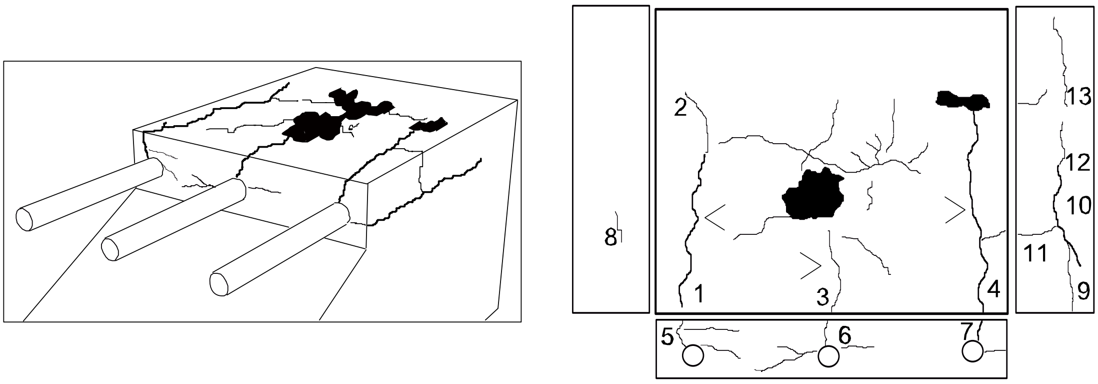

Specimen C2m2

Crack nr.	1	2	3	4	5	6	7	8	9	10	11	12	13
Width (mm)	0,4	0,2	0,1	0,3	0,2	0,15	0,15	0,05	0,1	0,3	0,25	0,25	0,1

Figure 5.4 (continued): Level 2 Crack patterns and width measurements.

5.3 Corrosion Level 3

The ongoing corrosion process at this level reached up to a maximum around 20% corrosion (Table 5.5).

The crack patterns are depicted in Figure 5.5. The formation of delamination planes was initiated in most specimens. The opening of the longitudinal cracks on the bottom cover slowed down, as will be shown further in the following section 5.4.

Table 5.5 Specimens for load test at Level 3.

Level	Specimen (^)	weight loss (%)	average attack (mm)	position (°)
3	B3(c)	10,9 (*)	560	left
		11,6 (*)	590	central
		12,9 (*)	660	right
	B3(m1)	13.0	671	left
		14.8	768	central
		13.5	699	right
	B3(m2)	15.7	820	left
		14.0	724	central
		9.2	473	right
	C3(c)	11.1	570	left
		16.7	872	central
		7.0	359	right
	C3(m1)	20,7 (*)	1100	left
		19,1 (*)	1010	central
		21,0 (*)	1110	right

(*) Corrosion calculated using Faraday's law.
(°) Front view with bars on the top (corrosion setup).
Note: see Section 5.5 for corrosion attack measurements

B) Specimens with stirrups

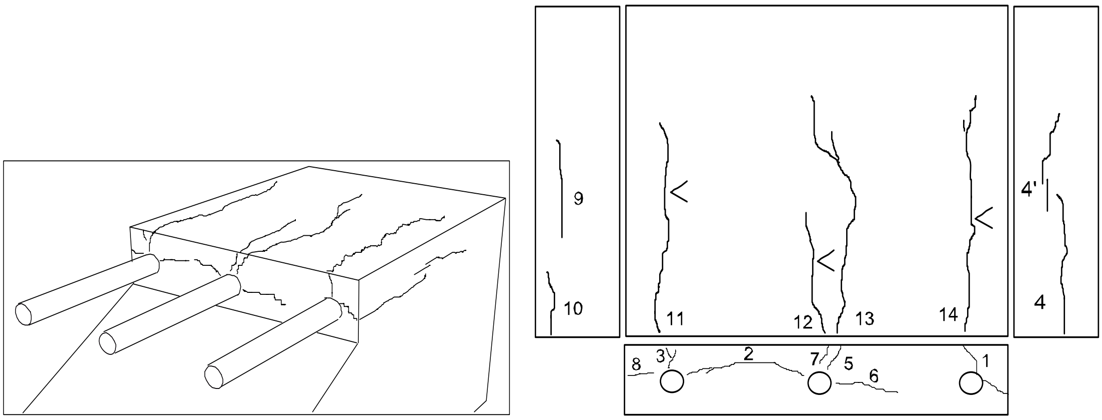

Specimen B3m1

Crack nr.	1	2	3	4	4a	5	6	7	8	9	10
Width (mm)	0.4	0.4	0.5	0.4	0.3	0.2	0.5	0.2	0.1	0.3	0.1
Crack nr.	11	12	13	14							
Width (mm)	0.6	0.2	0.2	0.4							

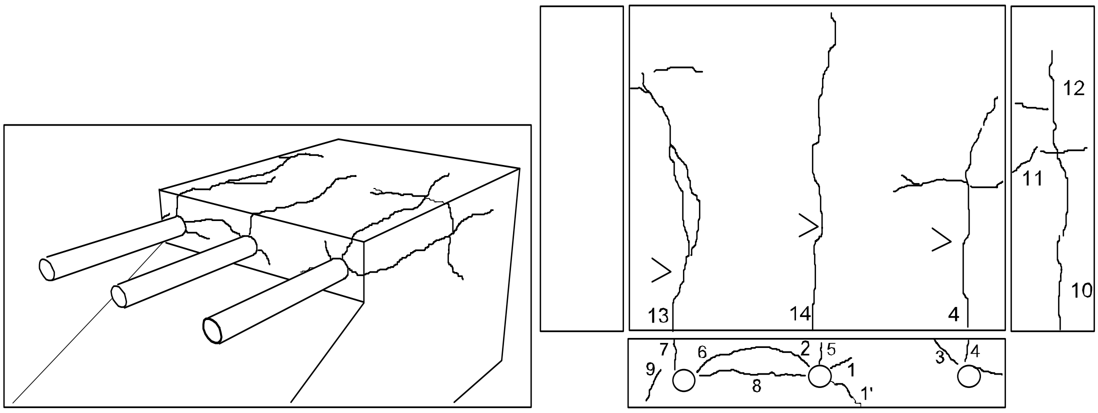

B3m2

Crack nr.	1	1’	2	3	4	5	6	7	8	9	10
Width (mm)	0.3	0.3	0.4	0.2	0.4	0.4	0.3	0.5	0.3	0.2	0.35
Crack nr.	11	12	13	14							
Width (mm)	0.35	0.3	0.4	0.25							

Figure 5.5 Level 3 crack patterns and width measurements.

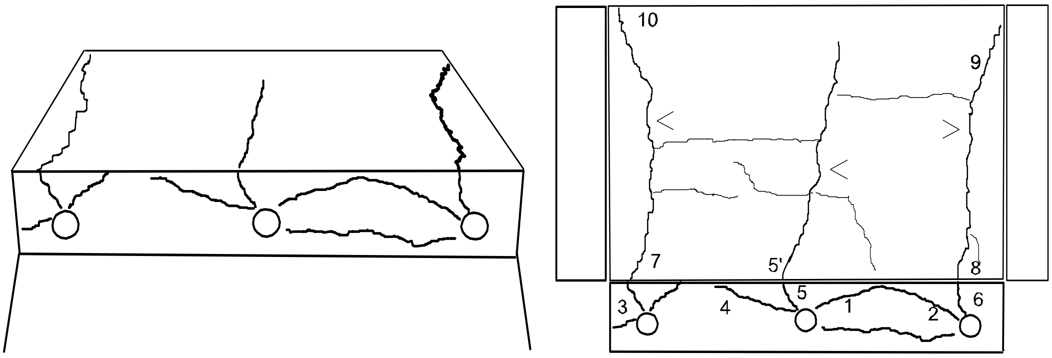

Specimen B3c

Crack nr.	1	2	3	4	5	5’	6	7	8	9	10
Width (mm)	0.40	0.20	0.50	0.3	0.2	0.1	0.5	0.4	0.35	0.3	0.2

C) Specimens with corroding stirrups

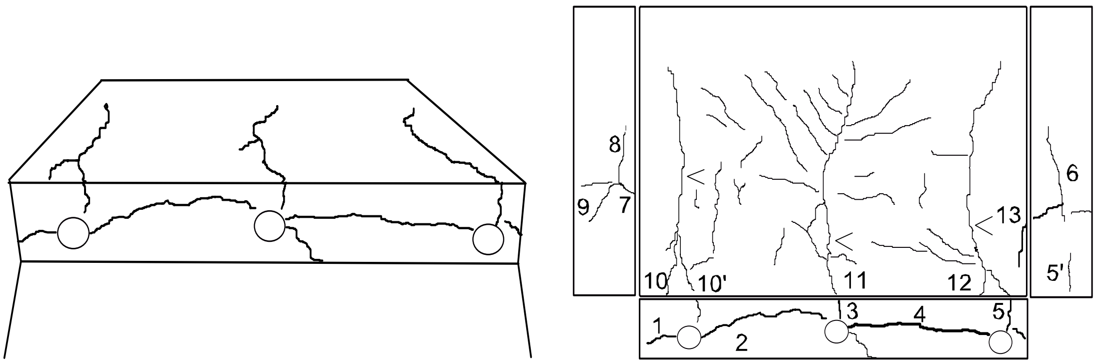

Specimen C3m1

Crack nr.	1	2	3	4	5	5’	6	7	8	9	10	11	12	13
Width (mm)	0.3	0.3	0.35	0.40	0.25	0.2	0.15	0.35	0.15	0.3	0.15	0.1	0.1	0.35

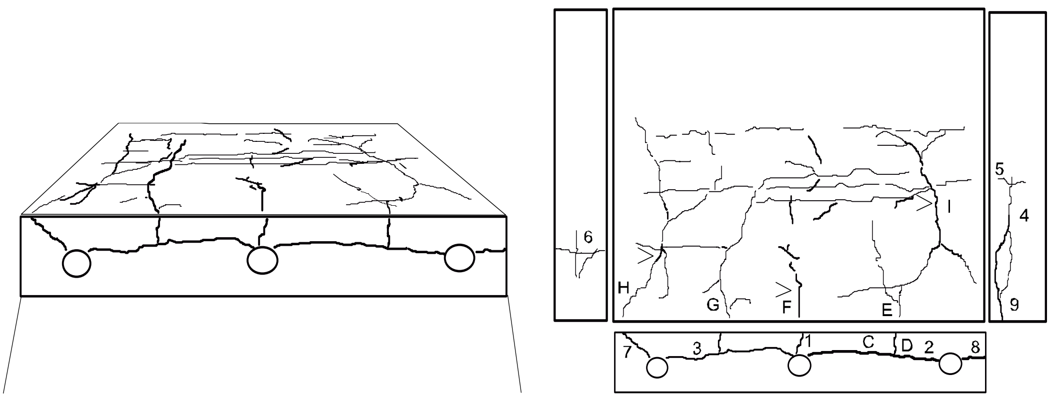

Specimen C3c

Crack nr.	1	2	3	4	5	6	7	8	9
Width (mm)	0,30	0,30	0,30	0,35	0,20	0,15	0,30	0,45	0,35
Crack nr.	C	D	E	F	G	H	I		
Width (mm)	0,45	0,20	0,25	0,20	0,15	0,20	0,30		

Figure 5.5 (continued) Level 3 crack patterns and width measurements.

5.4 Crack-corrosion diagrams

This section shows diagrams relating the corrosion crack widths and the corrosion of the reinforcement at the different levels.

The cracks are the longitudinal cracks in the top cover. Three crack width values and the corresponding corrosion levels are given for each diagram:

- the first crack opening;
- the maximum width reached in Level 1: the crack widths were measured in correspondence of the first crack location;
- the maximum opening (Levels 2 or 3 depending on the specimen) in correspondence of the locations indicated in the following.

The corrosion level in correspondence of each point is the average attack value for the whole bar calculated from the circulated current at level 1 and from gravimetric measurements at levels 2 or 3.

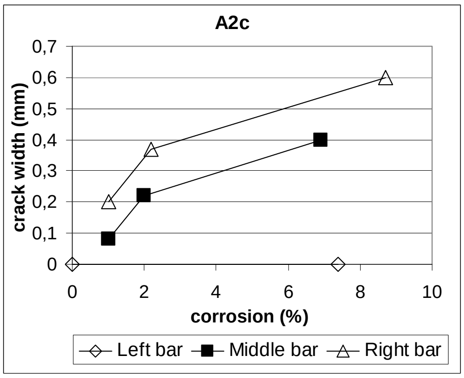

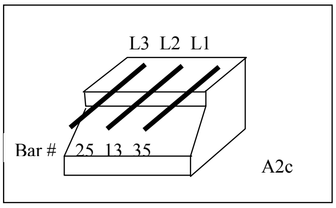

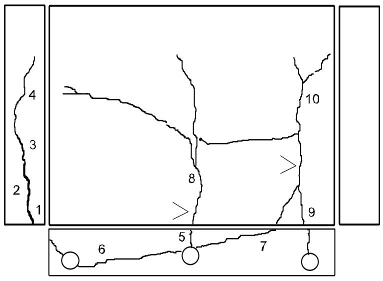

A2c		left bar			middle bar			right bar	
		bar # 25			bar # 13			bar # 35	
crack # (level 3)			crack # - (*)			crack # 8			crack # 9
		%	mm		%	mm		%	mm
level = 1st cracking					1	0.08		1	0.2
level 1		0	0		2	0.22		2.2	0.37
level 2		7.4	0		6.9	0.4		8.7	0.6

(*) no crack on the top cover

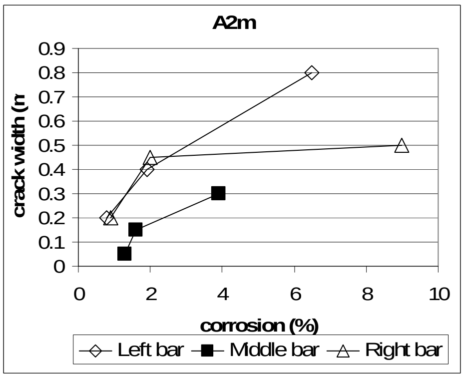

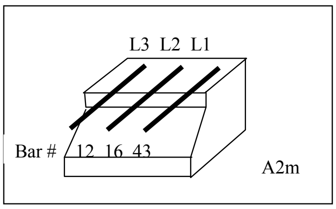

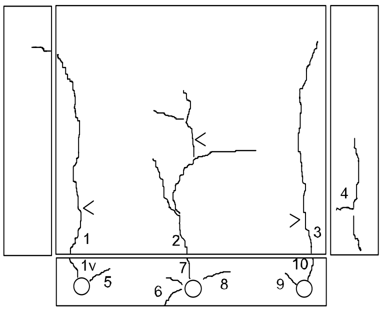

A2m		left bar			middle bar			right bar	
		bar # 12			bar # 16			bar # 43	
			crack # 1			crack # 2			crack # 3
		%	mm		%	mm		%	mm
level = 1st cracking		0.8	0.2		1.3	0.05		0.9	0.2
level 1		1.9	0.4		1.6	0.15		2	0.45
level 3		6.5	0.8		3.9	0.3		9	0.5

Figure 5.6 Crack-corrosion diagrams and synthesis of results (opening, level 1, 2 and 3).

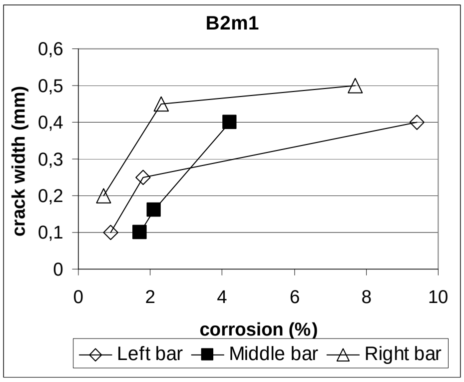

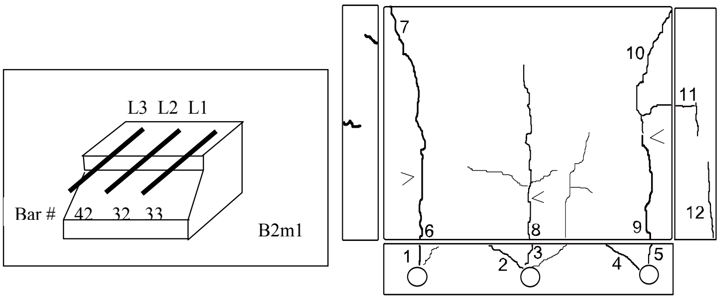

B2m1		left bar			middle bar			right bar	
		bar # 42			bar # 32			bar # 33	
crack # (level 3)			crack # 6			crack # 8			crack # 9
		%	mm		%	mm		%	mm
level = 1st cracking		0.9	0.1		1.7	0.1		0.7	0.2
level 1		1.8	0.25		2.1	0.16		2.3	0.45
level 3		9.4	0.4		4.2	0.4		7.7	0.5

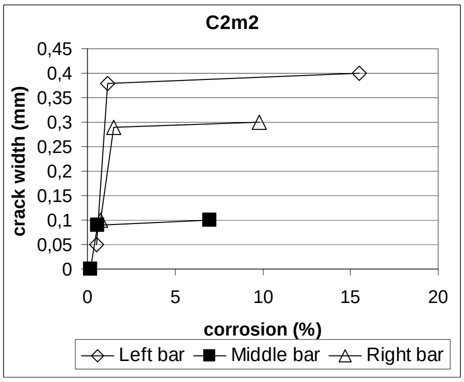

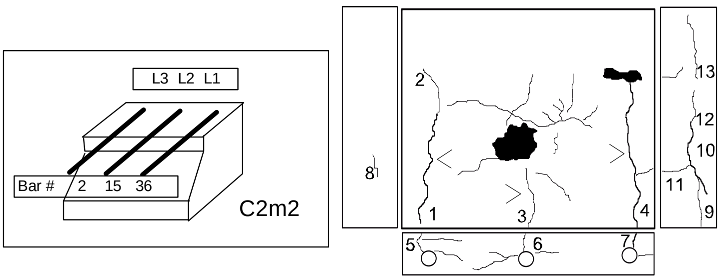

C2m2		left bar			middle bar			right bar	
		bar # 2			bar # 15			bar # 36	
crack # (level 3)			crack # 1			crack # 3			crack # 4
		%	mm		%	mm		%	mm
level = 1st cracking		0.5	0.05		0.168	0		0.75	0.1
level 1		1.15	0.38		0.56	0.09		1.5	0.29
level 3		15.5	0.4		7	0.1		9.8	0.3

Figure 5.6 (continued): Crack-corrosion diagrams and synthesis of results (opening, level 1, 2 and 3).

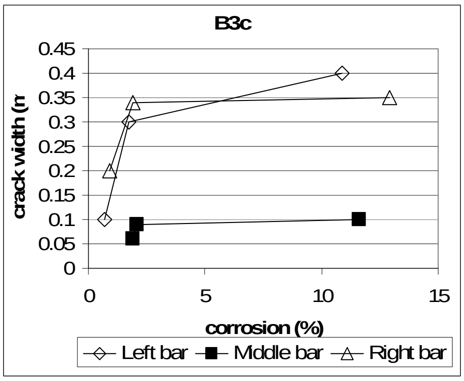

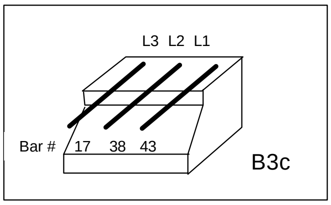

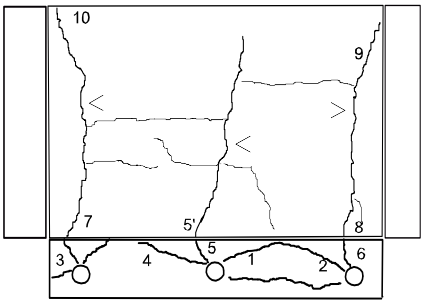

B3c		left bar			middle bar			right bar	
		bar # 17			bar # 38			bar # 43	
crack # (level 3)			crack # 7			crack # 5'			crack # 8
		%	mm		%	mm		%	mm
level = 1st cracking		0.7	0.1		1.9	0.06		0.9	0.2
level 1		1.75	0.3		2.1	0.09		1.9	0.34
level 3		10.9	0.4		11.6	0.1	610	12.9	0.35

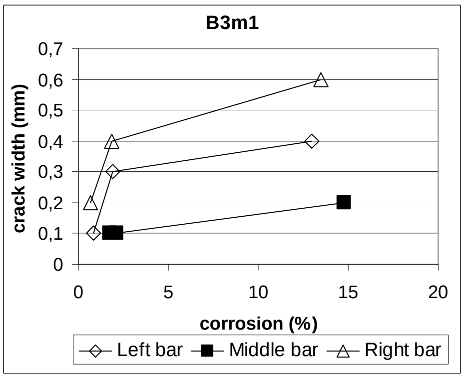

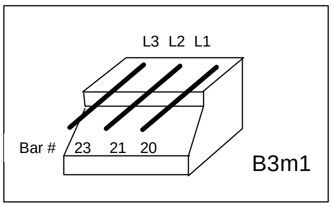

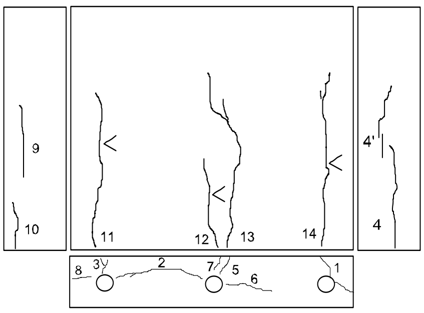

B3m1		left bar			middle bar			right bar	
		bar # 23			bar # 21			bar # 20	
crack # (level 3)			crack # 11			crack # 12			crack # 14
		%	mm		%	mm		%	mm
level = 1st cracking		0.85	0.1		1.74	0.1		0.7	0.2
level 1		1.9	0.3		2.15	0.1		1.85	0.4
level 3		13	0.4		14.8	0.2		13.5	0.6

Figure 5.6 (continued): Crack-corrosion diagrams and synthesis of results (opening, level 1, 2 and 3).

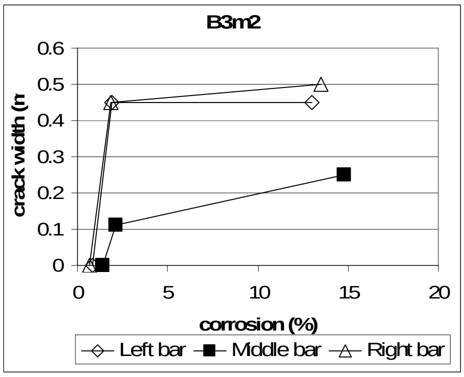

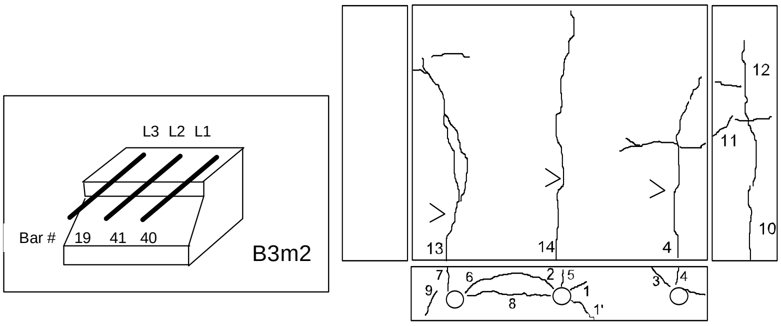

B3m2		left bar			middle bar			right bar	
		bar # 19			bar # 41			bar # 40	
crack # (level 3)			crack # 13			crack # 14			crack # 4
		%	mm		%	mm		%	mm
level = 1st cracking		0.762	0.1		1.4	0		0.84	0.2
level 1		1.9	0.45		2.15	0.11		1.85	0.45
level 3		13	0.45		14.8	0.25		13.5	0.5

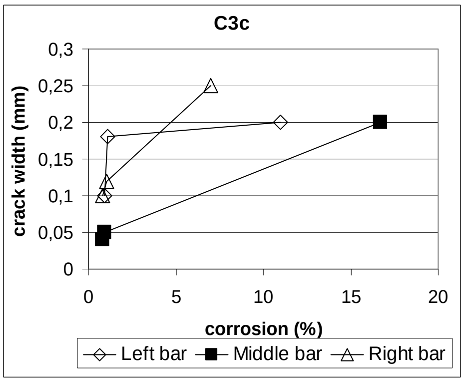

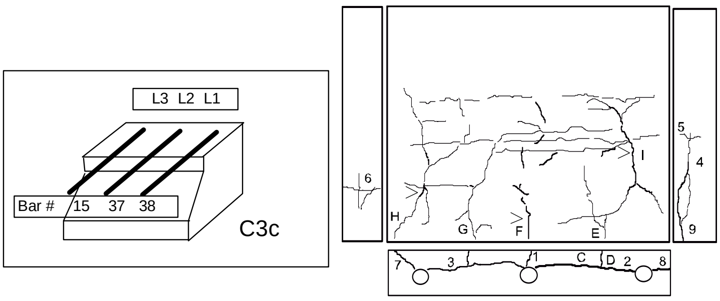

C3c		left bar			middle bar			right bar	
		bar # 15			bar # 37			bar # 38	
crack # (level 3)			crack # H			crack # F			crack # E
		%	mm		%	mm		%	mm
level = 1st cracking		0.94	0.1		0.8	0.04		0.82	0.1
level 1		1.11	0.18		0.9	0.05		1.05	0.12
level 3		11	0.2		16.7	0.2		7	0.25

Figure 5.6 (continued): Crack-corrosion diagrams and synthesis of results (opening, level 1, 2 and 3).

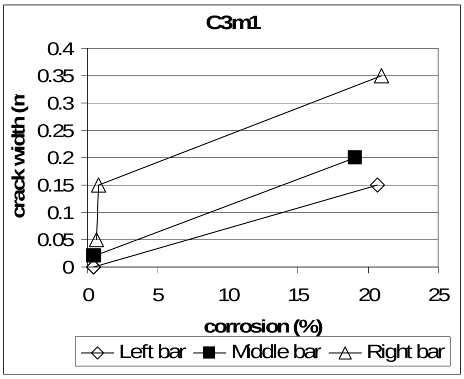

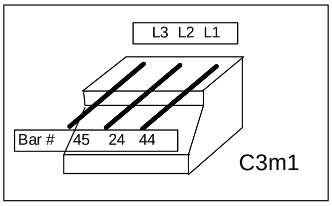

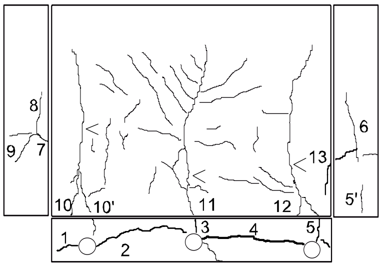

C3m1		left bar			middle bar			right bar	
		bar # 45			bar # 24			bar # 44	
crack # (level 3)			crack # 10			crack # 11			crack # 13
		%	mm		%	mm		%	mm
level = 1st cracking		0.4	0		0.43	0.02		0.623	0.05
level 1		0.4	0		0.5	0.02		0.8	0.15
level 3		20.7	0.15		19.1	0.2		21	0.35

Figure 5.6 (continued): Crack-corrosion diagrams and synthesis of results (opening, level 1, 2 and 3).

5.5 Corroded bars

The corrosion attack values were determined theoretically using Faraday's law and *a posteriori* by weight loss measurement. The difference between the two on average was approximately 10%.

The main reinforcement after the load testing were extracted from the concrete, breaking up the specimens. The maximum corrosion levels were measured by the weight loss measurements with the gravimetric method of the ISO 8407 standard. The results for all corroded bars are given in Table 5.6.

Typical results for weight measurements after the rust cleaning cycles (ISO 8407) for corroded bars are shown in Figure 5.7. The same procedure on non-corroded bars produced a weight loss of approximately 2 grams. The percentual loss for the corroded bars was then calculated with reference to the corroding length of 210mm of the 750mm long bars.

The corrosion level for one Type A and two Type C specimens was calculated only from the circulated current, because these specimens will be subjected to mechanical testing later and thus have not yet been broken up.

The bars were corroded mainly over half of the surface, in the part facing the lower cover at the top of the specimen, where the cathode was positioned (Figure 5.8). In specimen type B the protection of the stirrups with insulating tape proved to be efficient (Figure 5.9).

In specimens type C the stirrups were corroded (Figure 5.10). The examination of the corrosion cracks breaking up specimen C3c with corroded stirrups after the load tests (Figure 5.10) highlighted the presence of a delamination plane originating from stirrup corrosion, running across the corroding stirrups and isolating the portion of concrete covering the stirrups.

The corrosion of the stirrups (Table 5.7) was measured by the gravimetric method for specimen C3c, and using Faraday's law for the other specimens assuming that the whole surface of the stirrups was corroding, along the horizontal portion of the stirrups close to the cover and for a length of the vertical legs reaching at the level of the main bars. This assumption was based on the experimental observation of the corroded reinforcement (Figure 5.10). As a consequence, over the total surface through which the imposed current was flowing 45% was the stirrup surface and 55% the main bars.

Examples of the morphology of the corroded bars surface are shown in Figure 5.11. Both uniform reduction of the cross section and pitting are visible. The rib profile is smoothed.

Table 5.6 Corrosion attack, results of gravimetric measurements.

Level	Specimen	Rebar no	Weight (gr)	Weight corroded (gr)	loss (W-Wo)/Wo	average attack (micron)	position (°)
1	**B1c**	31	1826.0	1808.2	3.5	176	left
1	**B1c**	28	1811.5	1804.2	1.4	72	central
1	**B1c**	3	1815.5	1814.5	0.2	10	right
1	**B1m2**	22	1809.0	1807.9	0.2	11	left
1	**B1m2**	48	1820.0	1816.3	0.7	36	central
1	**B1m2**	29	1818.0	1807.5	2.1	104	right
2	**A2c**	25	1807.5	1770.5	7.3	372	left
2	**A2c**	13	1824.0	1780.6	8.5	434	central
2	**A2c**	35	1827.5	1781.9	8.9	456	right
2	**A2m**	12	1815.0	1778.2	7.2	369	left
2	**A2m**	16	1813.5	1790.6	4.5	228	central
2	**A2m**	34	1820.5	1774.8	9.0	459	right
2	**B2m1**	42	1830.5	1766.9	12.4	641	left
2	**B2m1**	32	1820.5	1799.3	4.2	210	central
2	**B2m1**	33	1814.5	1775.3	7.7	394	right
2	**C2m2**	2	-	-	9,8 (*)	500	left
2	**C2m2**	15	-	-	7,0 (*)	350	central
2	**C2m2**	36	-	-	15,5 (*)	810	right
3	**B3c**	17	-	-	10,9 (*)	560	left
3	**B3c**	38	-	-	11,6 (*)	590	central
3	**B3c**	43	-	-	12,9 (*)	660	right
3	**B3m1**	23	1818.5	1752.5	13.0	671	left
3	**B3m1**	21	1822.5	1747.1	14.8	768	central
3	**B3m1**	20	1833.0	1763.8	13.5	699	right
3	**B3m2**	19	1823.0	1742.7	15.7	820	left
3	**B3m2**	41	1817.0	1746.0	14.0	724	central
3	**B3m2**	40	1819.0	1772.0	9.2	473	right
3	**C3c**	38	1819.0	1783.1	7.0	359	left
3	**C3c**	37	1813.0	1728.3	16.7	872	central
3	**C3c**	15	1817.5	1761.1	11.1	570	right
3	**C3m1**	45	-	-	20,7 (*)	1100	left
3	**C3m1**	24	-	-	19,1 (*)	1010	central
3	**C3m1**	44	-	-	21,0 (*)	1110	right

(^) Mark: Specimen type (A, B, C) – Final Corrosion level (1, 2, 3) – Bar to be loaded in bond tests (c = corner; m = middle) – Specimen nr. (1, 2).

(*) Calculated from the circulated current.

(°) Front view with bars on the top (corrosion setup)

Table 5.7 Corrosion levels - Stirrups

Specimen	weight loss (%)	attack (mm)	Level	position (*)	notes
C2m2	12	0,25	2	-	calculated
C3m1	23	0,48	3	-	calculated
C3c	13	0,27	3	Front	measured
	24	0,51		Central	
	27	0,57		Central	
	34	0,75		Back	

(*) Front and back relative to loaded end of bar in scheme

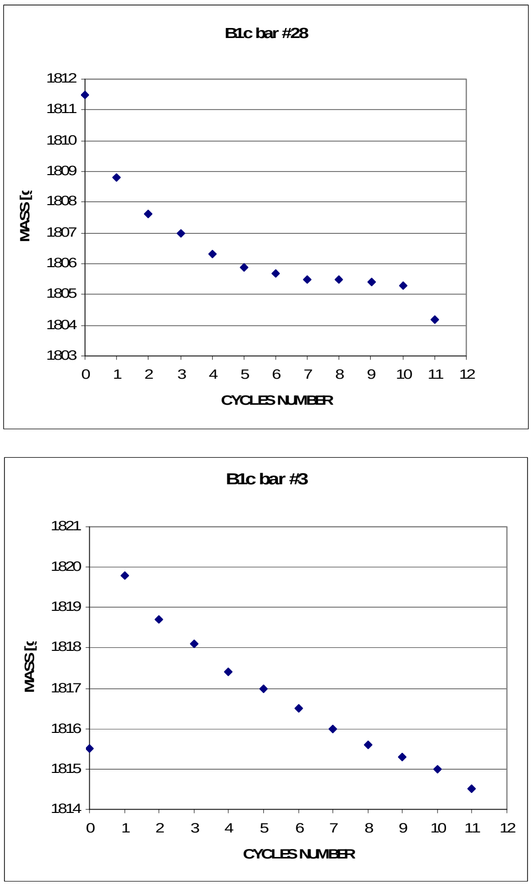

Figure 5.7 Gravimetric measurements for repeated cycles (ISO 8407).

Figure 5.8 The corrosion attack of the main bars from the bottom.

Protection of the stirrups from corrosion:

Figure 5.9 Type B specimens: uncorroded stirrup surface, after removing the protection tape.

(a)

(b)

(c)

(d)

(e)

(f)

Figure 5.10 Stirrup corrosion in specimen C3c: (a, c, d) Partial breaking of the cover due to the load test on the specimen; (b) cover removed by hammering and pneumatic drilling; (e-f) corroded stirrups exposed by drilling the surrounding concrete.

Figure 5.11 Morphology of the corroded bar surface.

Figure 5.11 (continued): Morphology of the corroded bar surface.

6 Pull-out test results

6.1 Failure mode

Different types of crack patterns at failure were observed depending of the level of corrosion and presence or absence of stirrups; see Figure 6.1:

(a) failure of the test specimen: inclined cracks starting from the bottom support towards the top supports; this occurred in only one specimen of type B with small corrosion penetration;

(b) splitting-induced pull-out failure: cracks running along the bar and turning parallel to the inclined side of the “nose”; this developed mostly in noncorroded specimens; and

(c) splitting failure: splitting cracks parallel to the bar, mainly in corroded specimens.

Failure of the test specimen (F) | Splitting-induced pull-out failure (SP) | Splitting failure (P)

Figure 6.1 Crack patterns at different failure modes observed in tests.

6.2 Bond strength

An overview of the test results in terms of bond strength for corroded reinforcement is presented in Figure 6.2. The bond strengths of the eccentric pull-out specimens were normalized with respect to that of the middle bar in reference specimens; this was done separately for the specimens with and without stirrups.

In general, the average bond strength of specimens with stirrups was less influenced by corrosion compared to that of the specimens without stirrups. This shows the importance of the confinement provided by stirrups after cover cracking. In the reference specimens without stirrups, the corner bars showed about a 25% lower bond strength than the middle bars; a larger difference, over 50%, in bond deterioration of the corner and middle bars was seen in the corroded specimens. A small effect of the bar position was seen in the presence of stirrups, both in reference and corroded specimens. The large bond deterioration seen in the corroded specimens without stirrups agrees well with what has been observed in pull-out tests by other researchers, see Almusallam *et al.* (1996), Fang *et al.* (2004) and Lee *et al.* (2002); a reduction of about 50% in bond strength for a corrosion level of about 5% weight loss has been reported.

As can be seen in Figure 6.2 (a), there was a relatively large bond deterioration in specimens with stirrups for small corrosion penetrations, up to about 5% weight loss. No significant bond deterioration was observed for larger corrosion attacks. An explanation can be that the pressure around the bar suddenly decreased in specimens with small corrosion penetration when the concrete cover cracked. However, for larger corrosion penetrations, the cracks were filled with rust and resulted in an increased pressure around the bar. Therefore, when a pull-out load was applied, it was not only the stirrups that provided confinement; the pressure around the bar due to accumulated rust also contributed to a higher bond capacity. Similar behaviour has been seen in pull-out tests carried out on specimens with stirrups, see Fang *et al.* (2004). These authors measured no substantial bond reduction in specimens corroded up to a 6% weight loss. The bond strength of the middle bar is slightly smaller than that of the corner bars; thus the stirrups provide more confinement to the corner bars, at the angle, than to the middle bars.

The average bond strength for each specimen is given in Table 6.1. The load measured on each bar was divided by the surface area of the bar along the embedment length to calculate the average bond stress. The types of the failures, i.e. failure of the test specimen (F), splitting-induced pull-out failure (SP) and splitting failure (S), were also reported in Table 6.1.

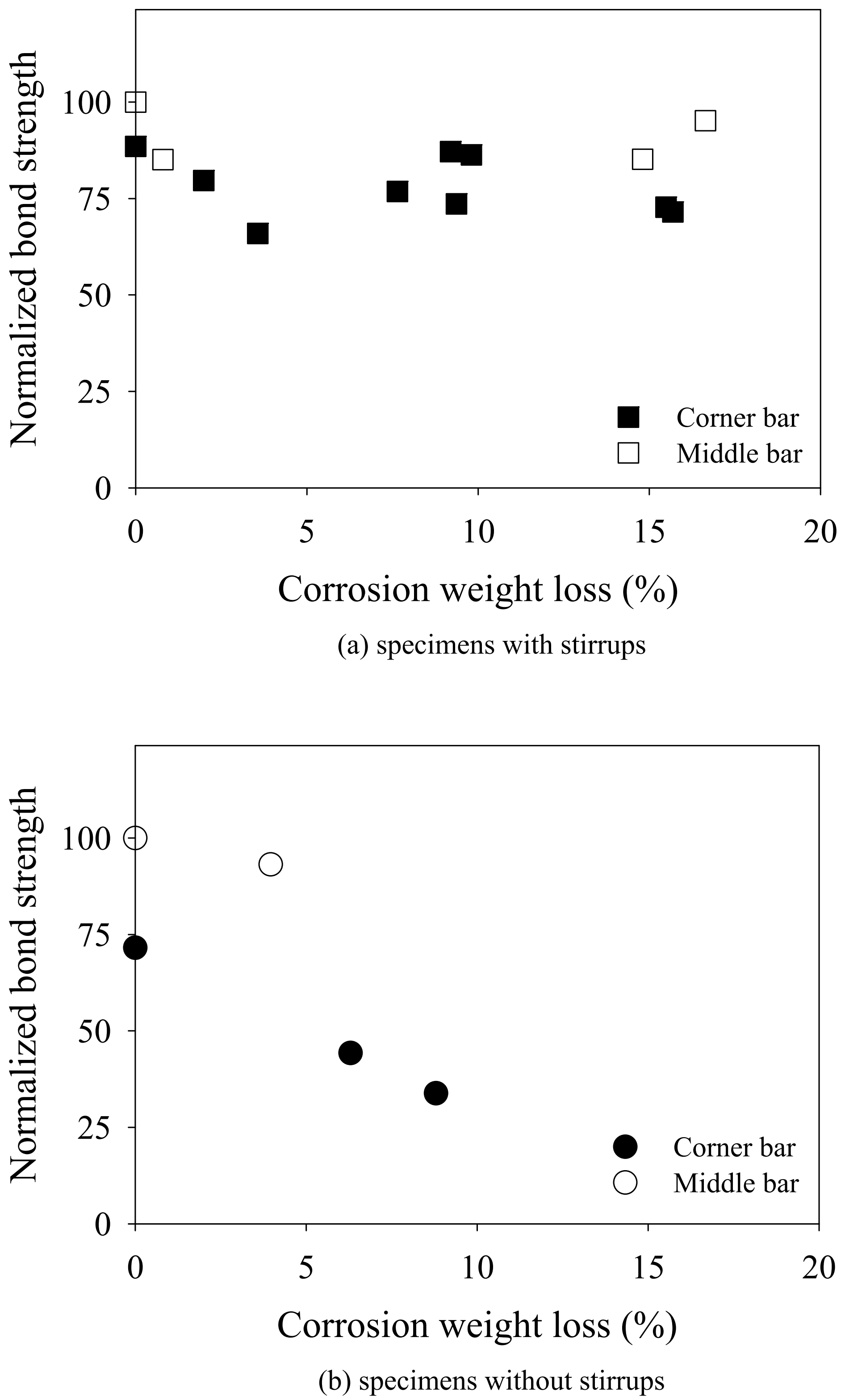

(a) specimens with stirrups

(b) specimens without stirrups

Figure 6.2 Overview of the test results in terms of bond strength normalized with respect to that of the middle bar in reference specimens, versus corrosion attack.

Table 6.1 Average bond strength, results from pull-out tests.

Corrsoin Level	Specimen	weight loss (%)	average attack (µm)	Position (°)	Bond τ_{max} (MPa)	Slip at τ_{max} (mm)	Failure mode
Reference	A0c	0	0	left	4.7	0.12	SP
		0	0	central	-	-	-
		0	0	right	4.9	0.13	SP
Reference	A0m	0	0	Left	-	-	-
		0	0	Central	6.71	0.17	SP
		0	0	right	-	-	-
Reference	B0c	0	0	left	7.81	0.41	SP
		0	0	central	-	-	-
		0	0	right	6.55	0.36	SP
Reference	B0m	0	0	left	-	-	-
		0	0	central	8.11	0.17	SP
		0	0	right	-	-	-
1	B1c	3.5	176	left	5.14	0.14	F
		1.4	72	central	-	-	-
		0.2	10	right	6.46	0.19	F
1	B1m2	0.2	11	left	-	-	-
		0.7	36	central	6.9	0.088	SP
		2.1	104	right	-	-	-
2	A2c	7.3	372	left	2.3	0.037	SP
		8.5	434	central	-	-	-
		8.9	456	right	3.0	0.025	S
2	A2m	7.2	369	left	-	-	-
		4.5	228	central	6.25	0.088	SP
		9.0	459	right	-	-	-
2	B2m1	12.4	641	left	6.23	0.7	S
		4.2	210	central	-	-	-
		7.7	394	right	5.8	0.16	S
2	C2m2	9,8 (*)	500	left	7.0	0.091	SP
		7,0 (*)	350	central	-	-	-
		15,5 (*)	810	right	5.92	0.057	SP
3	B3c	10,9 (*)	560	left	not tested		
		11,6 (*)	590	central			
		12,9 (*)	660	right			
3	B3m1	13.0	671	left	-	-	-
		14.8	768	central	6.91	0.081	SP
		13.5	699	right	-	-	-
3	B3m2	15.7	820	left	7.07	0.19	S
		14.0	724	central	-	-	-
		9.2	473	right	5.97	0.56	S
3	C3c	11.1	570	left	-	-	-
		16.7	872	central	7.72	0.059	SP
		7.0	359	right	-	-	-
3	C3m1	20,7 (*)	1100	left	not tested		
		19,1 (*)	1010	central			
		21,0 (*)	1110	right			

6.3 Bond versus crack width

Cracks are the first sign of damage to be visually observed in corroded concrete structures. It would be useful if the crack width could be used to estimate the influence of corrosion on the bond capacity. Therefore, to seek for such a relation, test results in terms of bond strength normalized with respect to that of the reference specimens versus total crack width are shown in Figure 6.3. The total crack width related to one corroded bar was calculate by adding the crack width of all longitudinal cracks originated from the corroded bar.

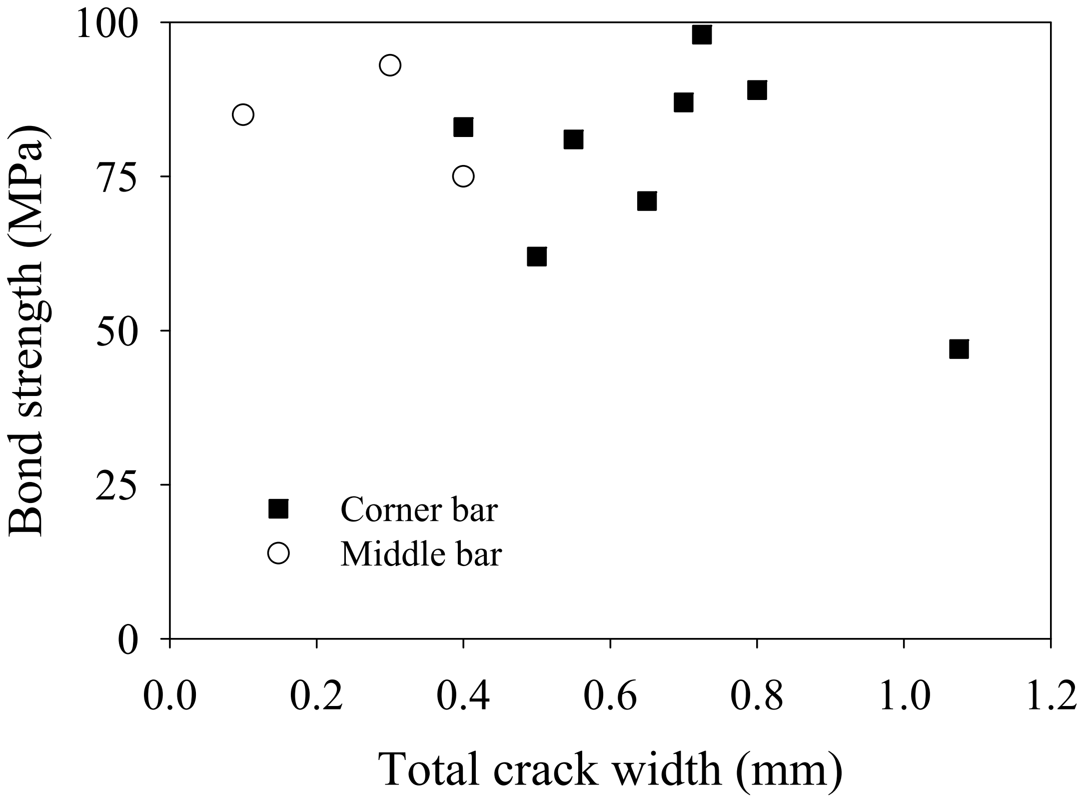

Figure 6.3 Overview of the test results in terms of bond strength normalized with respect to that of the middle bar in reference specimens, versus total crack width.

6.4 Bond stress versus slip

The average bond stress was plotted versus the slip at the free end; see Figure 10. The results given for the reference specimens are averages of at least two specimens; see Table 1. The numerical results in terms of bond stress versus slip are compared with those of the tests in Figure 6.4-Figure 6.12.

A comparison of the results of specimen types A, B and C shows the importance of the stirrups in the remaining bond capacity of corroded specimens. The largest bond deterioration was seen in the type A specimens on the corner bars; this was because of the absence of stirrups as well as less portion of surrounding concrete available to a corner bar compared to that of a middle bar. The least bond deterioration was measured in type B specimens on the corner bars. This is believed to be caused by the effective interaction between the stirrups and the main bars at the angle of the corner. It can be concluded that, for large corrosion penetrations that cause extensive cover cracking, stirrups play an important role in terms of being the main source of confinement.

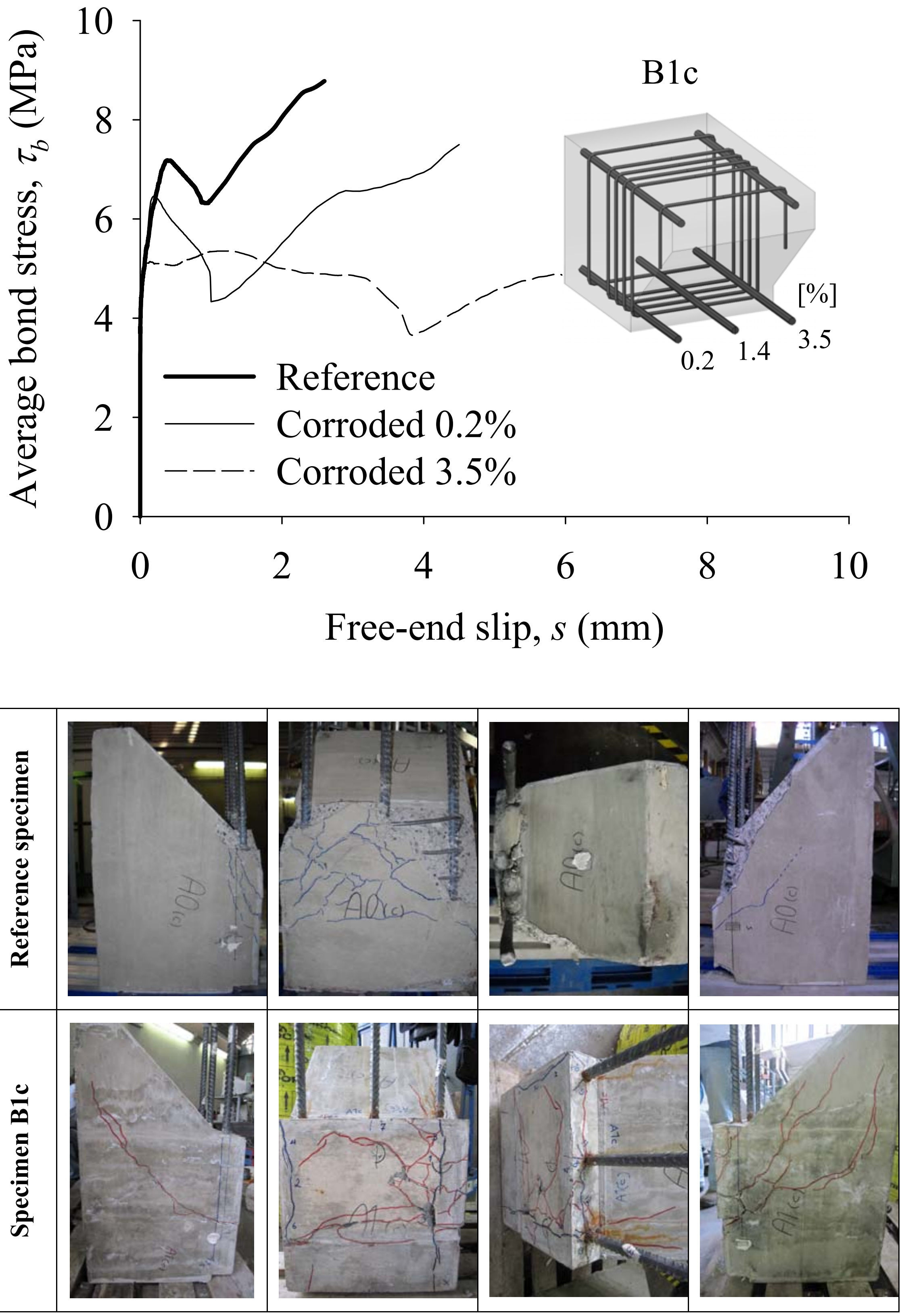

Figure 6.4 Average bond stress versus free-end slip measured in the pull-out tests for specimens B1c and the reference specimens.

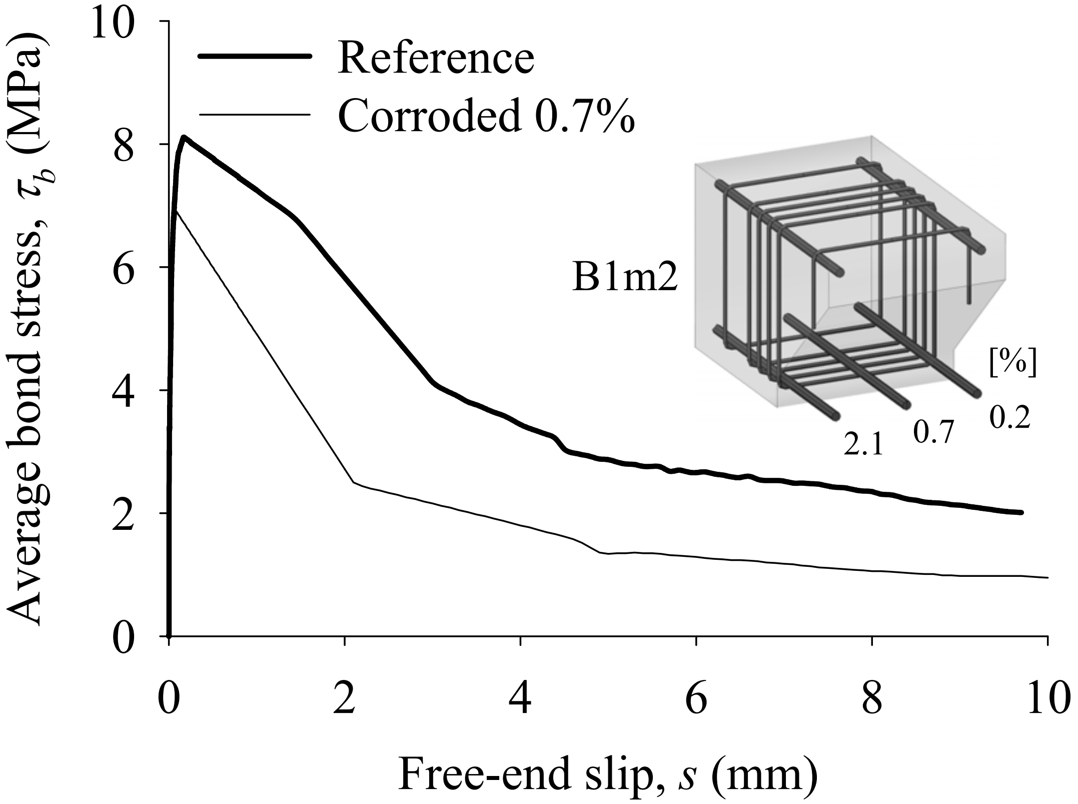

Figure 6.5 Average bond stress versus free-end slip measured in the pull-out tests for specimens B1m2 and the reference specimens.

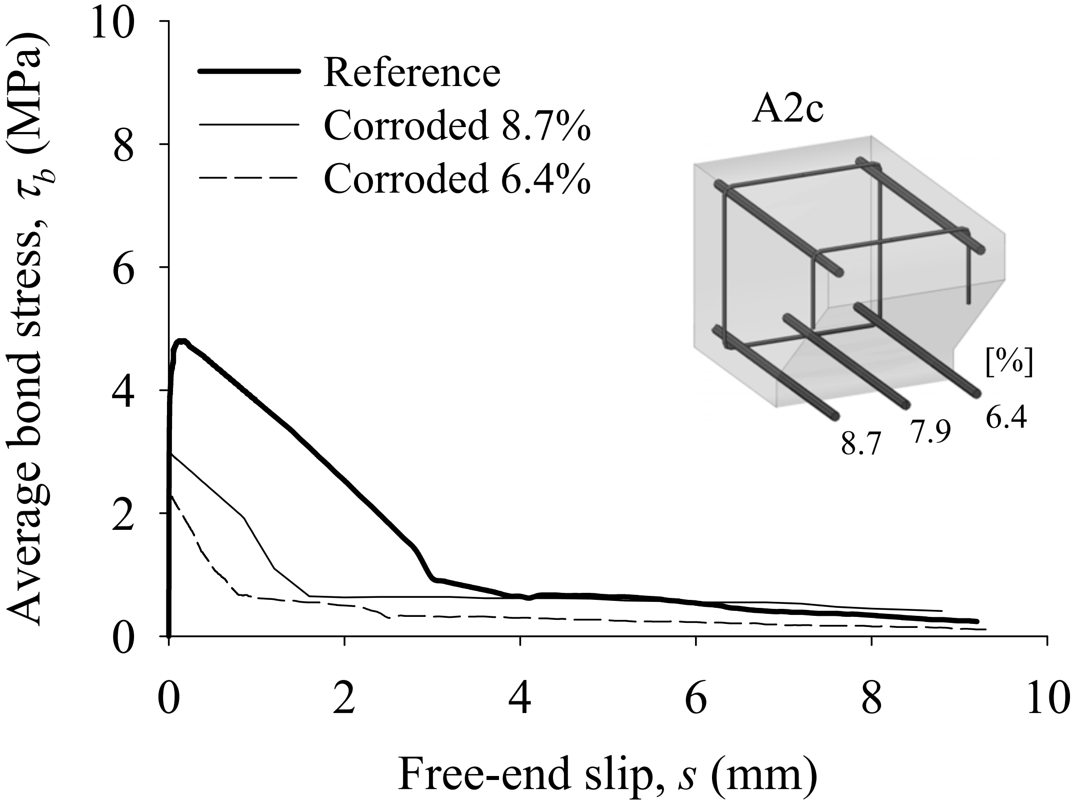

Figure 6.6 Average bond stress versus free-end slip measured in the pull-out tests for specimens A2c and the reference specimens.

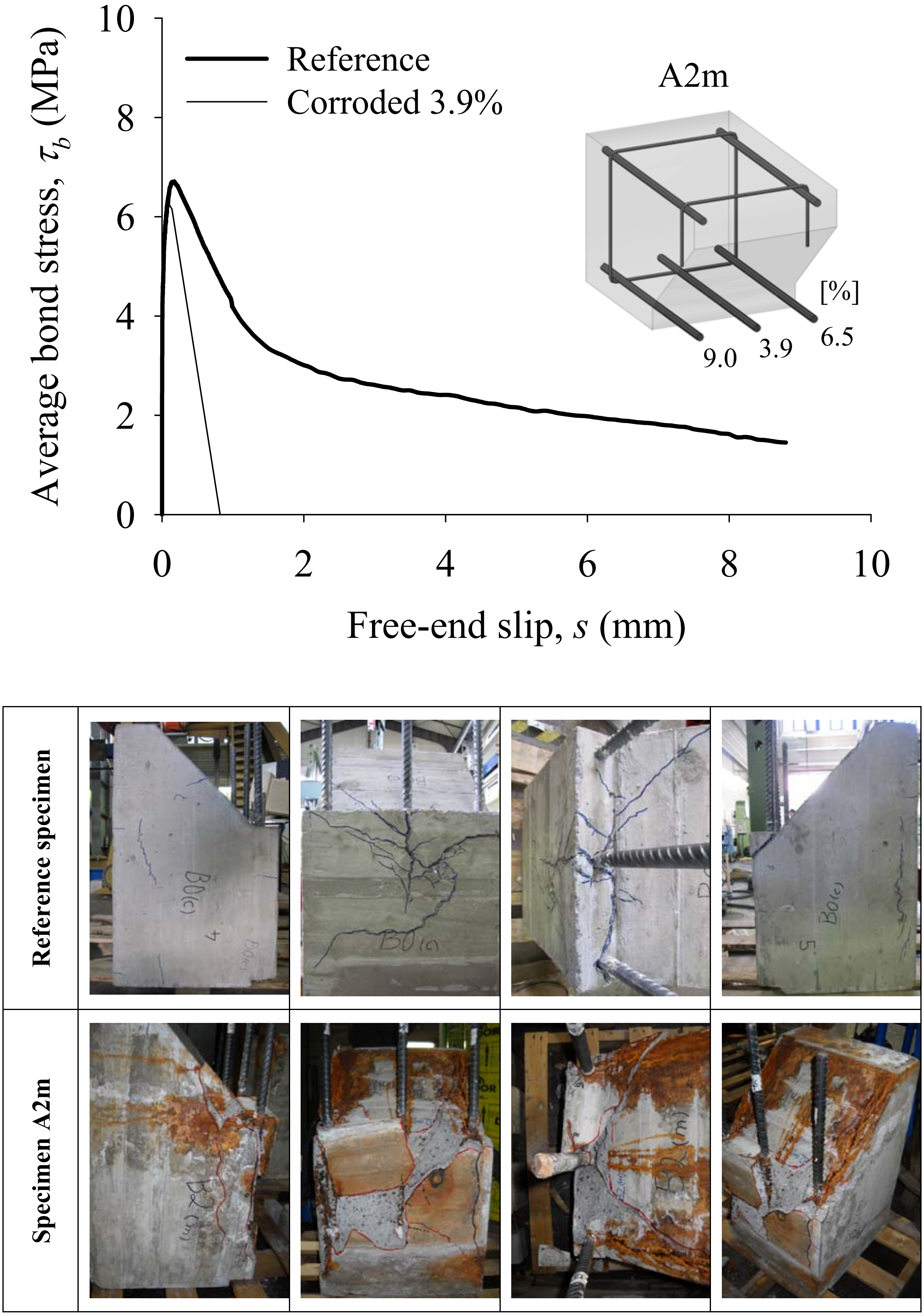

Figure 6.7 Average bond stress versus free-end slip measured in the pull-out tests for specimens A2m and the reference specimens.

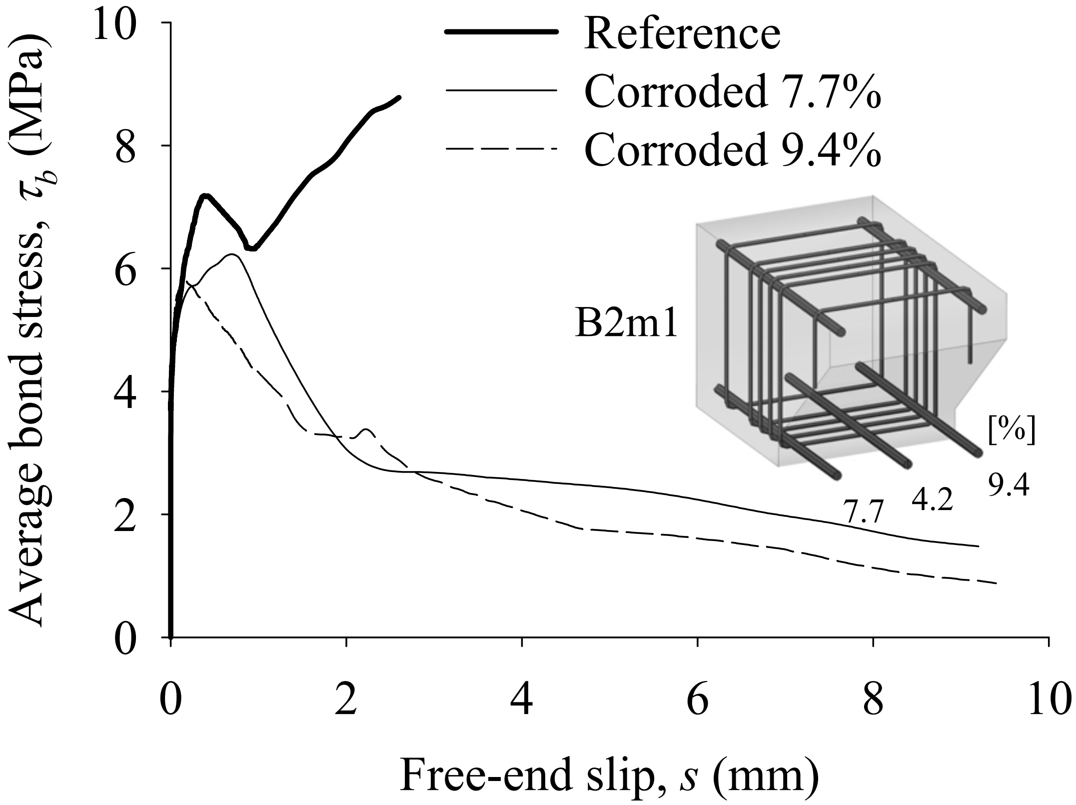

Figure 6.8 Average bond stress versus free-end slip measured in the pull-out tests for specimens B2m1 and the reference specimens.

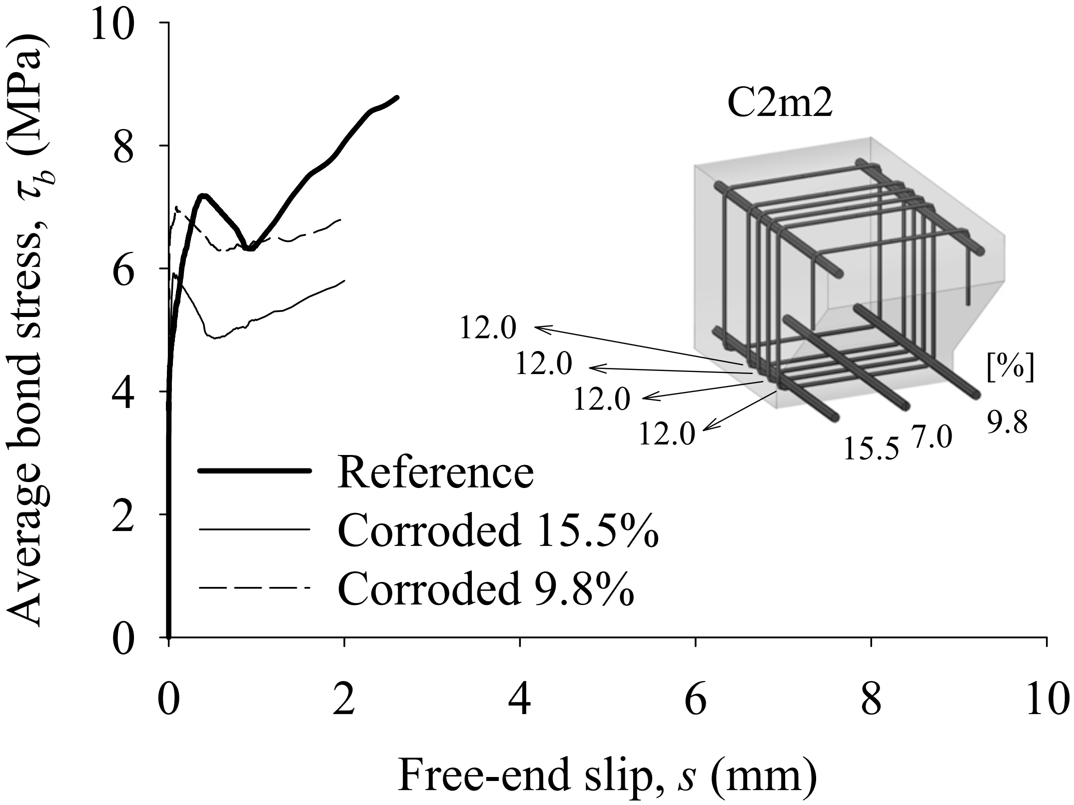

Reference specimen				
Specimen C2m2	no photo	no photo	no photo	no photo

Figure 6.9 Average bond stress versus free-end slip measured in the pull-out tests for specimens C2m2 and the reference specimens.

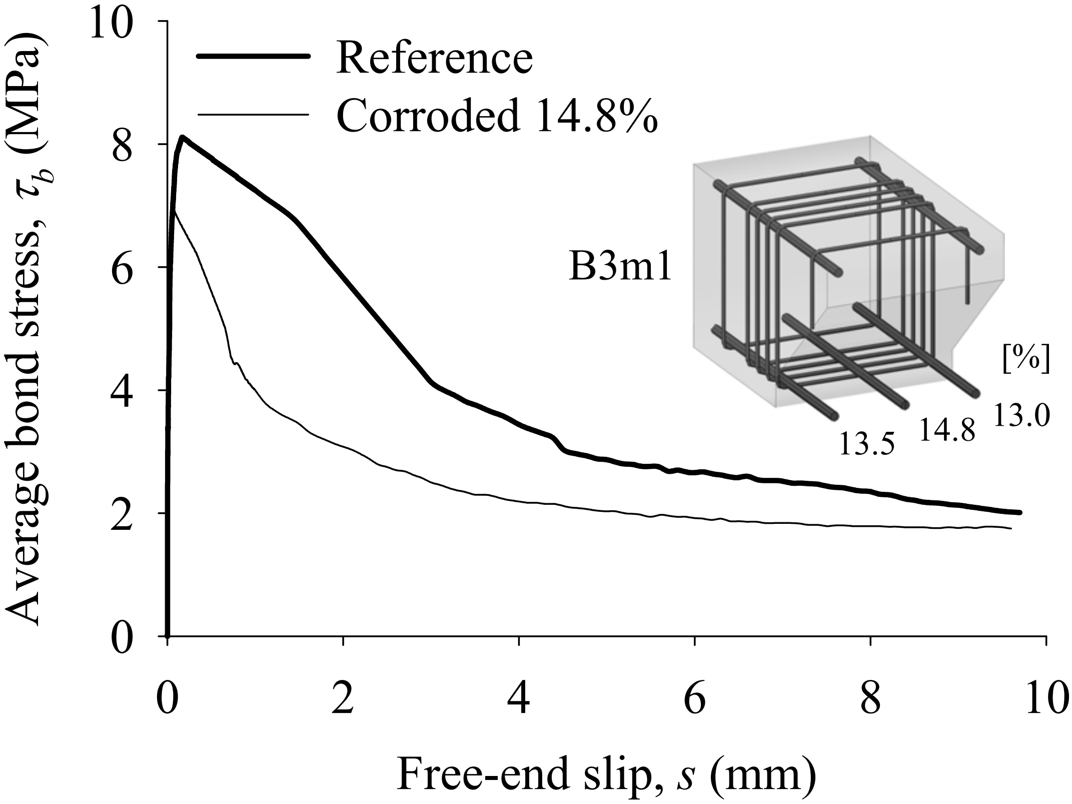

Figure 6.10 Average bond stress versus free-end slip measured in the pull-out tests for specimens B3m1 and the reference specimens.

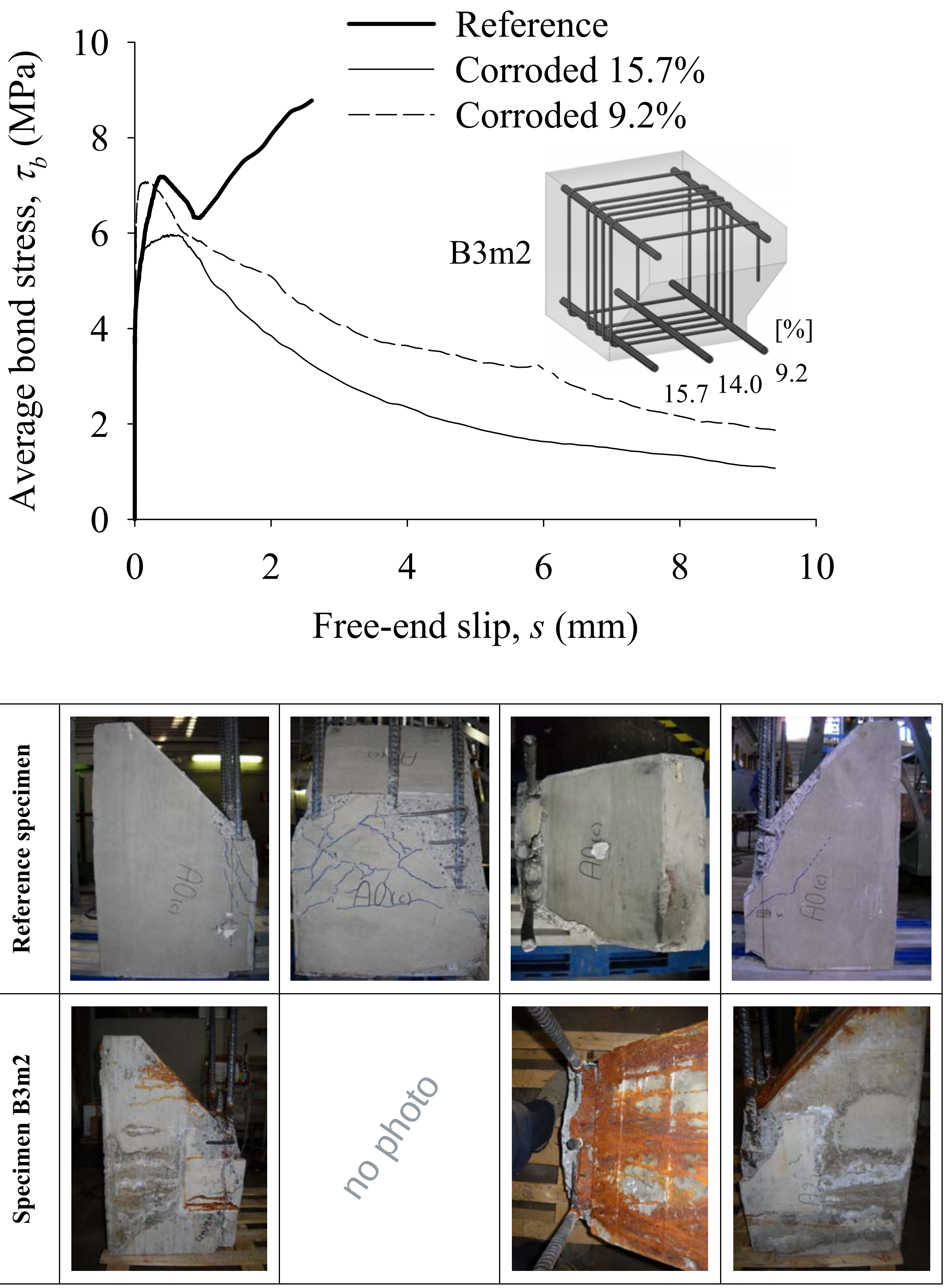

Figure 6.11 Average bond stress versus free-end slip measured in the pull-out tests for specimens B3m2 and the reference specimens.

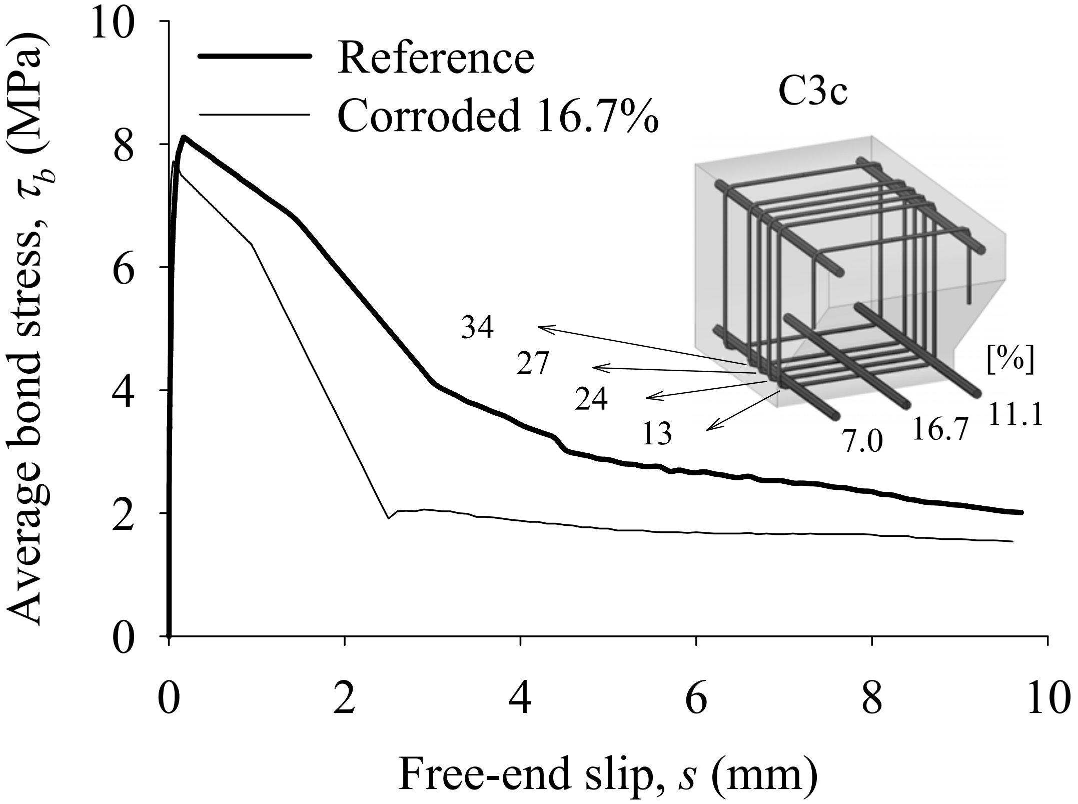

Reference specimen				
Specimen C3c	no photo	no photo	no photo	no photo

Figure 6.12 Average bond stress versus free-end slip measured in the pull-out tests for specimens C3c and the reference specimens.

6.4.1 Specimens type A: without stirrups

The bond strength of corner bars was considerably lower than that of the middle bars in the specimens without stirrups, Figure 6.6 and Figure 6.7; this was seen in both reference and corroded specimens. The pull-out tests on corner bars showed a roughly 50% reduction in bond strength caused by 8.7% corrosion. While less bond deterioration was observed in the pull-out tests on the middle bar, the failure was more brittle.

The cracking in reference specimens started with the development of a dominant longitudinal crack that appeared on both the bottom and side covers along the embedment length. This was followed by extensive inclined cracking that formed a splitting-induced pull-out failure. Corrosion in these specimens, prior to mechanical loading, led to a wide longitudinal crack along the embedment length. The crack appeared on both the bottom and side covers around a corroded bar in the corner region. This resembles a corner cover spalling situation; although the corner cover had not completely fallen off, as the amount of corrosion was relatively low. The longitudinal corrosion cracks were further opened while the bar was pulled out; no indications of inclined cracking were seen. The bond capacity was limited by spalling of the bottom cover that led to splitting failure. The failure was relatively brittle as no stirrups were present to provide confinement after cover spalling.

The crack pattern caused in pull-out tests of reference specimens showed a relatively local damage in the concrete around the bar. This means that the cracks originating from the tested bar did not reach the adjacent bar. However, in the pull-out tests of corroded specimens, the cracks initiating from the tested bar propagated towards the weaker zone at the adjacent corroded bars.

In two other studies, pull-out tests were carried out in specimens similar to the ones used in the present study, Clark and Saifullah (1993), Almusallam *et al.* (1996). The specimens had a prism shape and were cast without stirrups, with four bars arranged at the corners. In the study by Almusallam *et al.* (1996), a very high corrosion rate of about 3500 $\mu A/cm^2$ was used in artificial corrosion of the bars. Significant bond deteriorations of over 80% have been reported for corrosion levels greater than 6%. The bond deterioration measured in the other study by Clark and Saifullah (1993), in which a corrosion rate of 500 $\mu A/cm^2$ was adopted, compares well with the results of the current study. A bond loss of about 50% has been reported for a corrosion level of around 10% bar. It has also been observed that the corrosion level required to cause cover cracking increased for larger cover; however, the bond strength remained almost unaffected by variation of cover thickness.

6.4.2 Specimens type B: with stirrups

For the specimens with stirrups, see Figure 6.4, Figure 6.8 and Figure 6.11, the mechanism that limited the bond of corner bars was different from that observed in the middle bars of reference specimens, Figure 6.5 and Figure 6.10. There appeared to be a comparatively large increase in the pull-out force after the first peak in the corner bar tests. The cracking started in these specimens with the development of a transverse crack at the end of the embedment length. At a higher load, this crack propagated further and formed an inclined crack; this corresponds to the first peak. Greater pull-out forces were measured as the stirrups started to function effectively. This was combined with the initiation of several transverse cracks inclining toward the loaded end, forming a splitting-induced pull-out failure that corresponds to the final failure of the specimens. Meanwhile, longitudinal cracks, initiated from the loaded end, stopped when they reached the first stirrup.

The behaviour seen in the pull-out tests of corner bars is believed to be caused by the effective interaction between the main bars and the stirrups at the corner. A visual observation of the tests specimens after the pull-out tests showed a relatively large displacement of the stirrups at the corners; see Figure 6.13.

The pull-out tests of corner bars in corroded specimens showed relatively low bond deterioration and a different crack pattern at failure in comparison with the reference specimens. The failure of the corroded specimens was governed by spalling of the bottom cover; this formed a typical splitting crack pattern. A strong interaction between the adjacent bars was also seen in specimen type B. Thus, the corrosion-induced cracks reached the adjacent bars and facilitated spalling of the bottom cover in the pull-out tests.

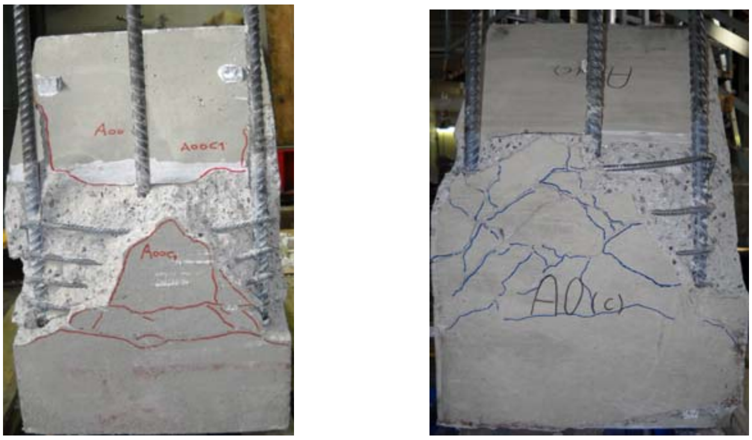

(a) (b)

Figure 6.13 Crack pattern after pull-out test of corner bars in tow reference specimens of type B.

6.4.3 Specimens type C: with corroded stirrups

In the specimens of type C, more extensive cracking, including several transverse cracks originating from corroded stirrups, was observed in both the tests and numerical analyses, Figure 5.6. The damage levels reached in corroded specimens did not show full delamination of the cover, although delamination cracks had started and propagated. To the knowledge of the authors, no available experimental laboratory study shows full delamination damage. The stirrups were highly corroded in the type C specimens; however, more than half of the cross section of the stirrups was still present.

The pull-out tests on specimens with corroded stirrups showed a comparatively low bond deterioration. It could be concluded that significant bond deterioration will start only when the level of stirrup corrosion is very high, e.g. more than 50%, approaching situations in which some stirrup legs are broken at some points of pitting and/or are nearly consumed by uniform corrosion. Regan and Kennedy Reid (2004) simulated a similar condition in the laboratory, in which beams were cast with shear reinforcement lacking the corner anchorages. A relatively large reduction in the capacity of the beams was observed, in spite of the fact that the effect of cover spalling as a result of stirrups corrosion was not taken into account, Regan and Kennedy Reid (2004). The level of stirrups and main bar corrosion measured in the specimens of the current study could correspond to the level of damage when the cover is delaminated. This is observed in real structures but has not yet been reproduced in the laboratory.

In general, relatively low bond deterioration was seen in the pull-out tests of corroded specimens with stirrups, even for large corrosion penetrations. A comparison of the results of specimen types A, B and C shows the importance of the stirrups in the remaining bond capacity of corroded specimens. The greatest bond deterioration was seen in the type A specimens on the corner bars; this was because of the absence of stirrups and a smaller portion of surrounding concrete available to a corner bar compared to that of a middle bar. The least bond deterioration was measured in specimens of type B on the corner bars. This is believed to be caused by the effective interaction between the stirrups and the main bars at the angle of the corner. It can be concluded that stirrups play an important role as the main source of confinement for large corrosion penetrations that cause extensive cover cracking.

The experimental work carried out by Higgins and Farrow III (2006) studied shear capacity of beams with corroded stirrups. A high corrosion rate of 600 $\mu A/cm^2$ was used to produce corrosion in stirrups; corrosion of the flexural reinforcement was prevented. They observed extensive cracking, partial delamination and staining at stirrups' sectional loss of 12%, 20% and 40%. They concluded that visual inspection of corrosion damage did not help to distinguish between the three corrosion levels. Considering the low corrosion rate used in the current study and the comparatively little damage seen in the specimens with corroded stirrups, it is concluded that the corrosion rate of stirrups affects the test results in the same way as the corrosion rate of the main bars. That is, the time to reach a corrosion level is considerably shortened with a high corrosion rate; thus, the flow of rust through cracks does not effectively take place. This is an important phenomenon that ought to be taken into account in experiments and numerical analyses dealing with high corrosion attacks.

7 Conclusion

An experimental program aiming at evaluation of the anchorage capacity in corroded concrete structures was carried out, investigating the effect of high corrosion levels, cover cracking and delamination, and corrosion of the stirrups. The test results of the artificial corrosion process and of the pull-out tests are presented in this report. Based on experimental observations the following conclusions are drawn.

Artificial corrosion:

- In the first phase of the tests, reaching approximately 1% corrosion, longitudinal cracks opened parallel to the main reinforcement, propagating in the direction of the lower cover.
- In the second phase, the conditions encountered in real highly corroded structures were studied. Even if the complete delamination of the cover did not occur in the tests, a partial propagation of the phenomenon was observed. One specimen with corroded stirrups was broken after the tests and the corrosion cracks examined; here, a delamination plane was clearly visible, running across the corroding stirrups and isolating the portion of concrete covering the stirrups. It can be concluded that the experimental damage pattern reproduced conditions observed in real structures, although the cover was not yet delaminated.
- This study shows that stirrup corrosion causes damage quite different from that occurring when stirrups are not corroded; this can be useful in linking the knowledge gained in laboratory corrosion tests to the damage observed in real structures. The most radical conclusions may be that tests without stirrup corrosion are not meaningful for an understanding of the behaviour of real structures. A more moderate conclusion is that, with corroded stirrups, the damage becomes more severe and diffuse than the damage that occurs when only the main bars corrode, which mainly causes longitudinal cracking. For a given level of corrosion of the main bars, the damage in a real structure with corroding stirrups is greater than is shown by tests without corroding stirrups.

Pull-out test:

- The test results showed the significant influence of the stirrups, the position of the tested bar and the corrosion on the bond capacity and the failure mode.
- Less bond capacity was observed for a bar positioned in a corner, which implies that the average confinement available for such a bar is less than that of a middle bar. The difference in the bond capacity, originating from the bar position, became even more important in the absence of stirrups.
- When the main bars were corroded, the highest anchorage capacity was measured for a middle bar in the presence of uncorroded stirrups, while the lowest capacity was measured for a corner bar in the absence of stirrups.
- A rather complex failure mode was observed in specimens with stirrups. This was a result of the effective interaction between stirrups and main bars at the angle of the corner. In the absence of stirrups, the failure of the corroded specimens was mainly governed by splitting of the concrete cover.

8 References

8407 (1991)

8407, I. (1991): *Corrosion of metals and alloys -- Removal of corrosion products from corrosion test specimens.* City, Place, xx-yy pp.

Almusallam, A. A., Al-Gahtani, A. S. and Aziz, A. R. (1996). Effect of reinforcement corrosion on bond strength. *Construction and Building Materials,* Vol. 10, No. 2, pp. 123-129.

Clark, L. A. and Saifullah, M. (1993): *Effect of corrosion on reinforcement bond strength.* Engineering Technical Press, City, Place, xx-yy pp.

Coronelli, D., Zandi Hanjari, K. and Lundgren, K. (2010). Severely corroded reinforced concrete with cover cracking. *submitted to Materials and Structures,* Vol. No. pp.

Fang, C., Lundgren, K., Chen, L. and Zhu, C. (2004). Corrosion influence on bond in reinforced concrete. *Cement and Concrete Research,* Vol. 34, No. 11, pp. 2159-2167.

fib (2000). *Bond of reinforcement in concrete, State-of-art report*. fib bulletin 10. Fédération internationale du béton, prepared by Task Group Bond Models.

Higgins, C. and Farrow III, W. C. (2006). Tests of reinforced concrete beams with corrosion-damaged stirrups. *Aci Structural Journal,* Vol. 103, No. 1, pp. 133-141.

Lee, H.-S., Noguchi, T. and Tomosawa, F. (2002). Evaluation of the bond properties between concrete and reinforcement as a function of the degree of reinforcement corrosion. *Cement and Concrete Research,* Vol. 32, No. 8, pp. 1313-1318.

Magnusson, J. (2000): *Bond and Anchorage of Ribbed Bars in High-Strength Concrete.* Ph.D. Thesis, Division of Concrete Structures, Chalmers University of Technology, Göteborg, 299.

Regan, P. E. and Kennedy Reid, I. (2004). Shear strength of RC beams with defective stirrup anchorages. *Magazine of Concrete Research,* Vol. 56, No. 3, pp. 159-166.

Sæther, I. (2009). Bond deterioration of corroded steel bars in concrete. *Structure and Infrastructure Engineering, First published on: 29 July 2009 (iFirst), DOI: 10.1080/15732470802674836*

Vol. No. pp.

Sæther, I., Antonsen, A. and Vennesland, Ø. (2007): *Effect of impressed anodic current density applied to accelerated corrosion laboratory results.* City, Place, xx-yy pp.

Saifullah, M. and Clark, L. A. (1994). Effect of corrosion rate on the bond strength of corroded reinforcement. *Proceedings of International Conference: CORROSION AND CORROSION PROTECTION OF STEEL IN CONCRETE.* University of Sheffield. 591-602.

Vidal, T., Castel, A. and FrancÌ§ois, R. (2004). Analyzing crack width to predict corrosion in reinforced concrete. *Cement and Concrete Research,* Vol. 34, No. 1, pp. 165-174.

Yuan, Y., Ji, Y. and Shah, S. P. (2007). Comparison of two accelerated corrosion techniques for concrete structures. *Aci Structural Journal,* Vol. 104, No. 3, pp. 344-347.

Zandi Hanjari, K. (2010a): *Structural Behaviour of Deteriorated Concrete Structures.* Department of Civil and Environmental Engineering, Chalmers University of Technology, Göteborg, 257.

Zandi Hanjari, K., Coronelli, D. and Lundgren, K. (2010b). Anchorage capacity of severely corroded bars with corroded stirrups. *submitted to Magazine of Concrete Research,* Vol. No. pp.

APPENDIX A Test specimen geometry

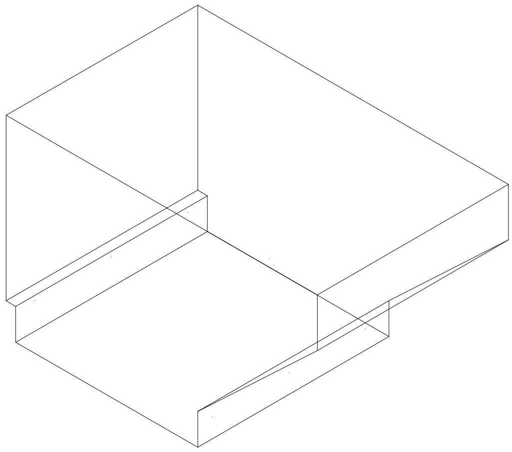

3D view

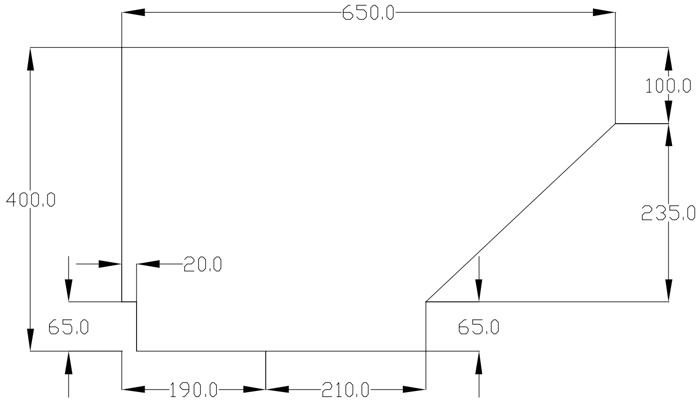

Side view

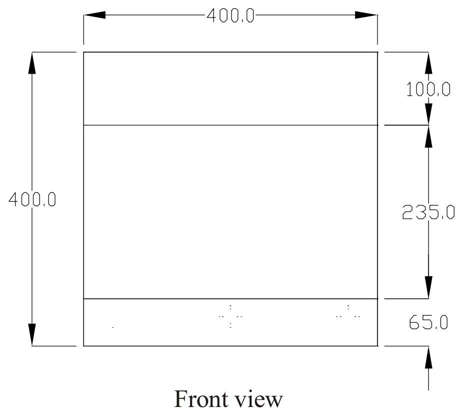

Front view

Figure A.1 Specimen Geometry of the beam-end specimens [mm]

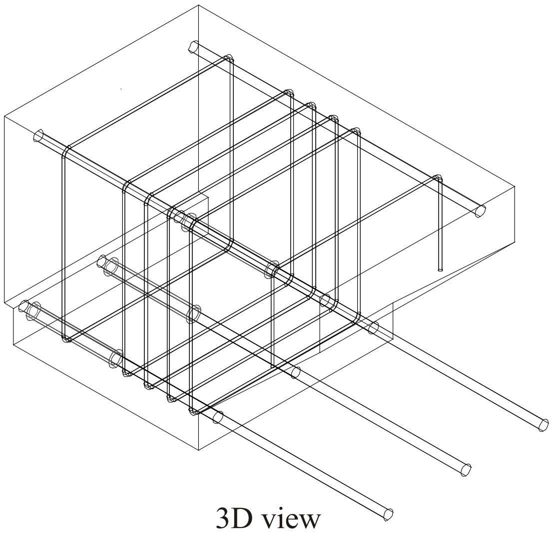

3D view

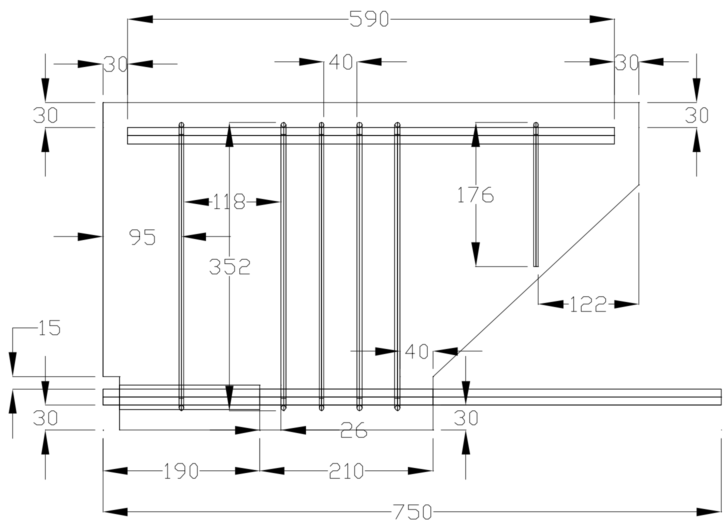

Side view

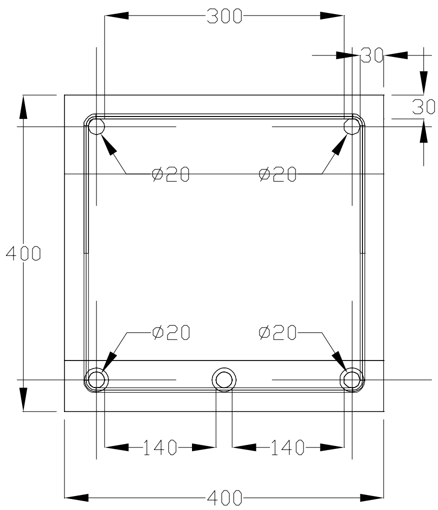

Front view

Figure A.2 Reinforcement detailing of the beam-end specimens with transverse reinforcement along the embedment length.

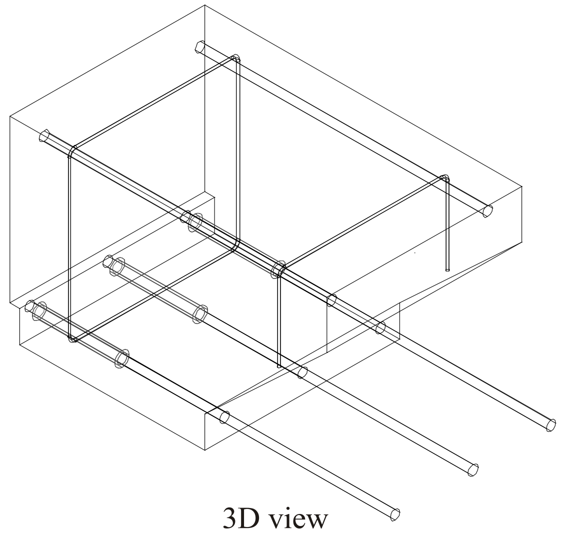

3D view

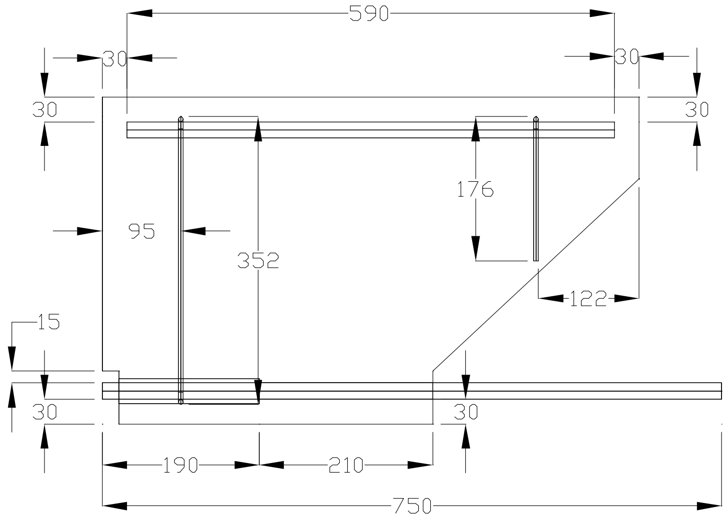

Side view

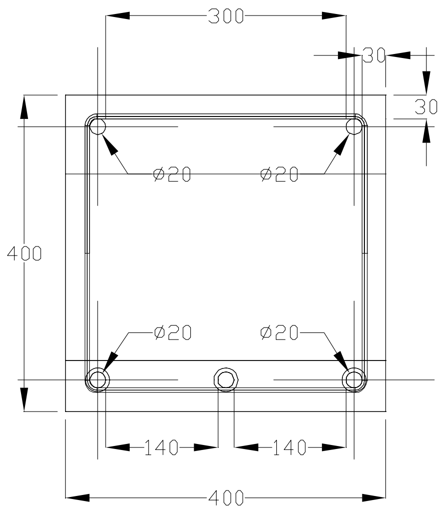

Front view

Figure A.3 Reinforcement detailing of the beam-end specimens without transverse reinforcement along the embedment length.

APPENDIX B Actual concrete cover

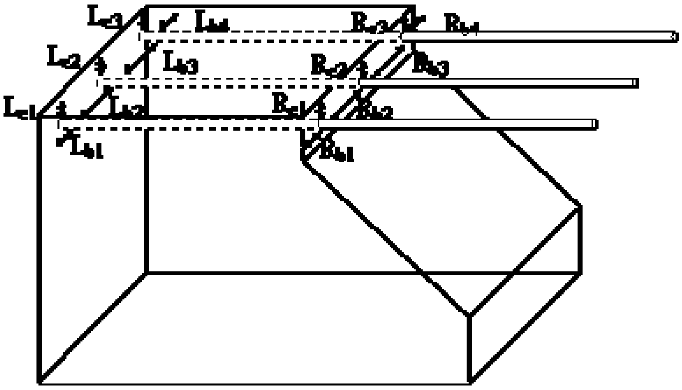

Table B.1 Actual bottom and side concrete cover.

Spec. ID	Front							Back						
	Lb1	Lb2	Lb3	Lb4	Lc1	Lc2	Lc3	Rb1	Rb2	Rb3	Rb4	Rc1	Rc2	Rc3
B0m	39	125	132	33	27	30	30	41	121	140	29	26	27	28
B0c	50	121	133	30	22	28	26	45	124	143	27	25	27	30
B3m1	47	126	136	28	27	29	27	39	124	136	27	26	29	28
B1m2	42	125	137	30	27	28	30	38	124	134	30	28	30	27
B1c	42	125	138	33	29	32	32	43	122	134	27	27	27	28
B2m1	46	122	131	26	29	32	29	42	125	140	29	32	32	29
B3m2	53	113	131	18	26	32	30	44	125	134	26	30	27	27
B3c	34	125	135	38	27	31	30	34	131	136	30	28	25	27
A0m	38	123	143	32	28	30	28	42	113	142	25	29	28	33
A0c	19	132	140	29	30	31	29	30	134	140	28	30	28	33
A2m	26	139	142	25	28	30	25	28	136	139	29	26	27	28
A2c	26	135	142	27	28	32	25	27	143	135	29	34	33	32
C3m1	41	121	132	38	28	29	27	38	123	144	27	27	20	26
C2m2	32	123	141	32	31	32	29	40	123	137	28	28	28	29
C3c	32	126	131	34	30	32	30	37	123	127	31	29	27	29

APPENDIX C Actual embedment length

Table C.1 Actual embedment length.

Spec. ID	Embedment length [mm]		
	l_{b1}	l_{b2}	l_{b3}
B0m	204	213	204
B0c	206	210	210
B3m1	210	210	210
B1m2	205	225	210
B1c	210	210	210
B2m1	210	207	207
B3m2	210	205	200
B3c	*	*	*
A0m	204	203	210
A0c	217	216	212
A2m	212	210	215
A2c	208	213	214
C3m1	210	215	210
C2m2	213	220	220
C3c	212	215	227

* not measured

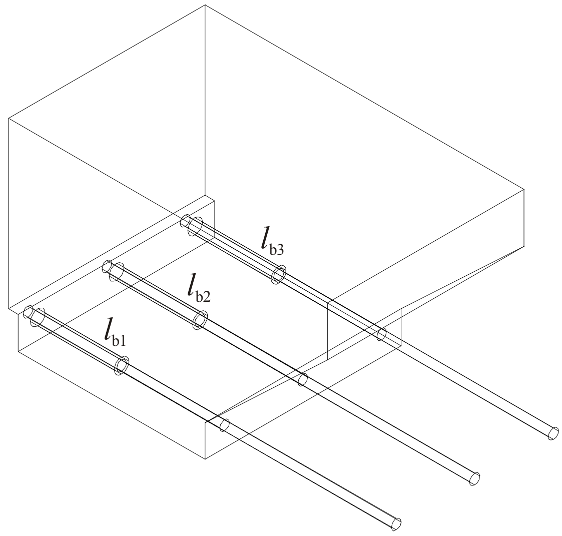

APPENDIX D Test setup

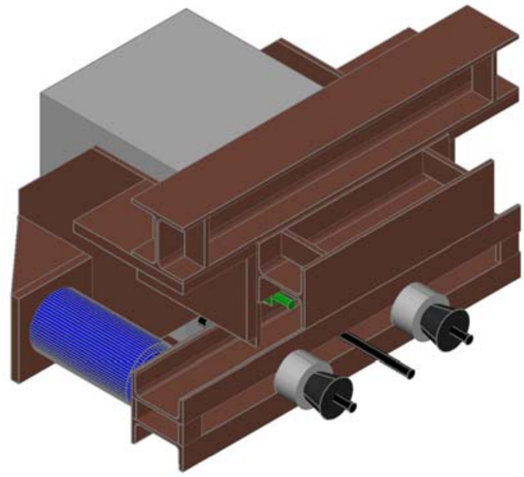

(a) 3D view: SE Isometric

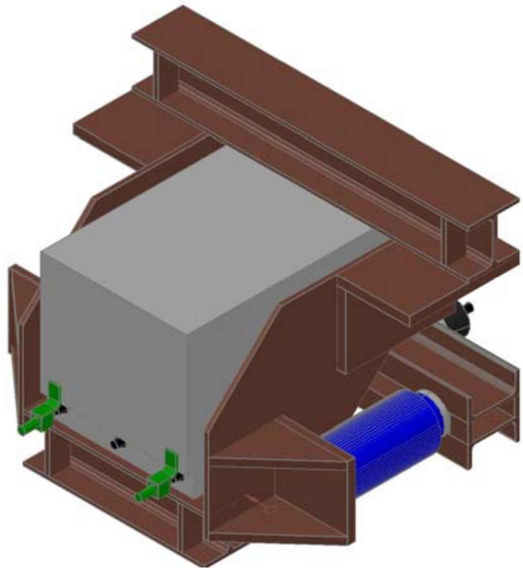

(b) 3D view: NE Isometric

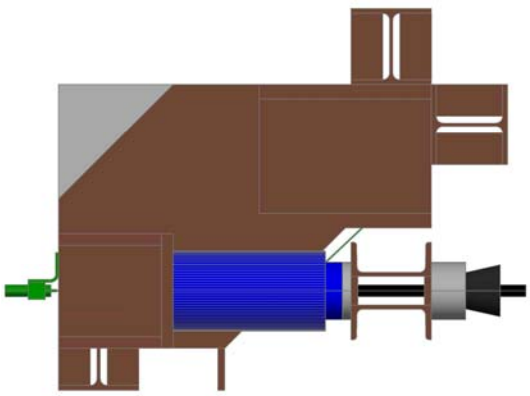

(c) Side view: right

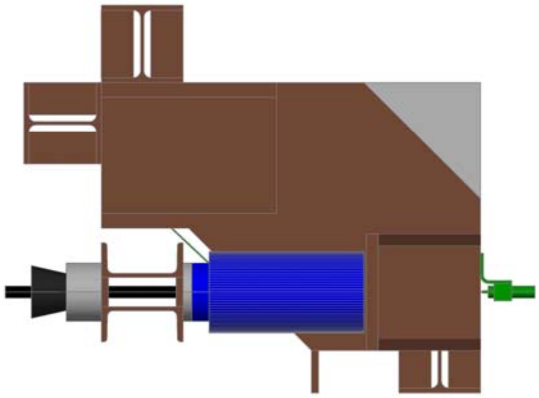

(d) Side view: left

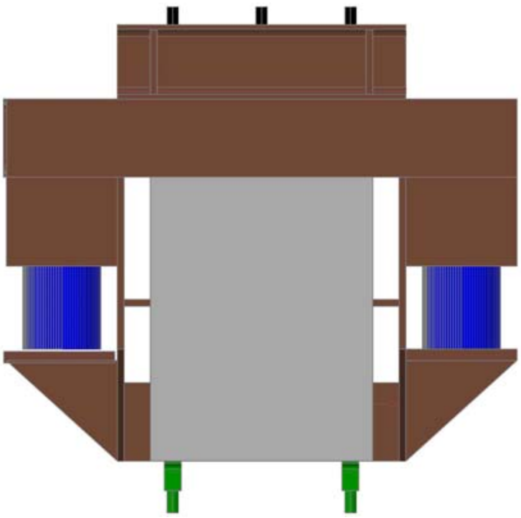

(e)Top view

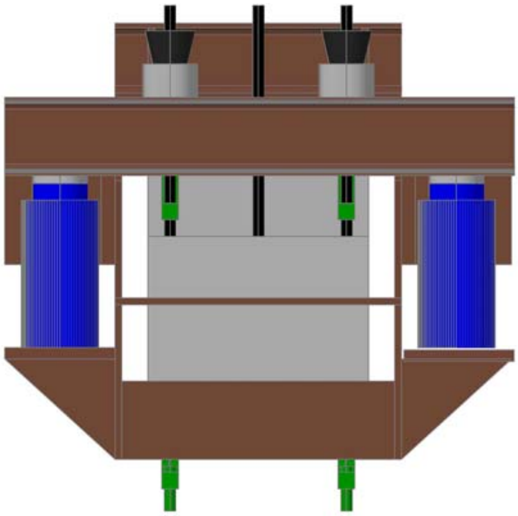

(f) Bottom view

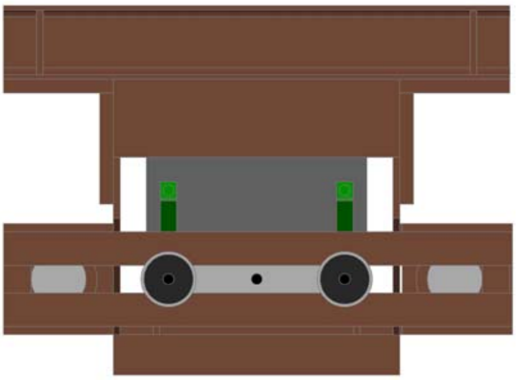

(g) Front view

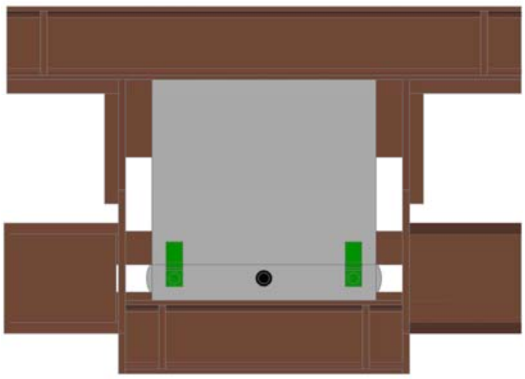

(h) Back view

Figure D.1 Drawings of the tests set-up

APPENDIX E Artificial corrosion and crack measurements - level 1

Date	18/11/2009

Specimen	Right Bar [mA]	Middle Bar [mA]	Left Bar [mA]	Total[mA]	Sum R+M+L [mA]
A2(m2)	4.7	5.5	4.5	17	14.7
A2(m1)	4.2	7	4.5	16.1	15.7
B2(m)	3.2	4.8	7.7	15.9	15.7
C2(m1)	1.38	1.55	0.65	15.9	3.58
A1(m1)	5.5	6	4.3	16.1	15.8
B2(c)	3.4	8.2	4.3	16.1	15.9
C2(c)	6.5	2.3	5.6	16.1	14.4
A2(c)	4.4	6.9	4.3	16.2	15.6
A1(c)	6.3	5.8	3.9	16.1	16
A1(m2)	5.1	5.3	4.6	15.8	15
C2(m2)	7.1	4.6	3.9	16.1	15.6

Data	30/11/2009

Specimen	Right Bar [mA]	Middle Bar [mA]	Left Bar [mA]	Total[mA]	Sum R+M+L [mA]
A2(m2)	5.5	6.2	5	17	16.7
A2(m1)	5	6.8	5.7	16.1	17.5
B2(m)	6	4.6	5.5	20	16.1
C2(m1)	1.8	2.3	0.8	20	4.9
A1(m1)	7.2	7	6.5	20	20.7
B2(c)	6.5	7.2	6.4	21	20.1

		average depth (μm)	average depth (μm)	average depth (μm)	crack (mm)	crack (mm)	crack (mm)
	Specimen	Right bar	Middle bar	Left bar	Right bar	Middle bar	Left bar
10/12/2009	A2(m2)	42.1	47.4	38.3	0.20	0.00	0.10
	A2(m1)	38.3	52.0	43.6	0.20	0.00	0.10
Time (days)	B2(m)	45.9	35.2	42.1	0.20	0.00	0.20
30	C2(m1)	13.8	17.6	6.1	0.00	0.00	0.00
	A1(m1)	55.1	53.6	49.7	0.17	0.10	0.05
	B2(c)	49.7	55.1	49.0	0.20	0.08	0.00

C2(c)	5	3.5	6.8	20	15.3
A2(c)	6	7.2	4.8	20	18
A1(c)	5.9	6.7	6.6	19	19.2
A1(m2)	5.2	4.8	5.9	18	15.9
C2(m2)	9	2	6	20	17

C2(c)	38.3	26.8	52.0	0.00	0.00	0.00
A2(c)	45.9	55.1	36.7	0.20	0.00	0.10
A1(c)	45.1	51.3	50.5	0.10	0.00	0.25
A1(m2)	39.8	36.7	45.1	0.20	0.00	0.10
C2(m2)	68.9	15.3	45.9	0.10	0.00	0.05

Data 14/12/2009

Specimen	Right Bar [mA]	Middle Bar [mA]	Left Bar [mA]	Total[mA]	Sum R+M+L [mA]
A2(m2)	5	6.8	5.1	18	16.9
A2(m1)	5.5	5	4.9	17	15.4
B2(m)	5.5	4	5.2	15	14.7
C2(m1)	5.5	2.5	2.5	15.5	10.5
A1(m1)	5.8	4.7	4.5	16	15
B2(c)	6.5	4.3	5	16	15.8
C2(c)	4.8	5.4	4.3	16.7	14.5
A2(c)	4.7	5.3	4.7	17	14.7
A1(c)	5	3.5	8.5	18	17
A1(m2)	5.5	3.5	5.1	17	14.1
C2(m2)	7	3.2	5	15.5	15.2

15/12/2009

Time (days)

5

	average depth (μm)	average depth (μm)	average depth (μm)	crack (mm)	crack (mm)	crack (mm)
Specimen	Right bar	Middle bar	Left bar	Right bar	Middle bar	Left bar
A2(m2)	48.5	56.1	44.8	0.25	0.05	0.20
A2(m1)	45.3	58.4	49.9	0.20	0.00	0.20
B2(m)	52.9	40.3	48.7	0.25	0.00	0.20
C2(m1)	20.8	20.8	9.3	0.00	0.00	0.00
A1(m1)	62.5	59.6	55.5	0.25	0.10	0.15
B2(c)	58.0	60.6	55.4	0.20	0.10	0.00
C2(c)	44.4	33.7	57.5	0.00	0.00	0.00
A2(c)	51.9	61.9	42.7	0.20	0.00	0.13
A1(c)	51.5	55.7	61.3	0.15	0.00	0.35
A1(m2)	46.8	41.2	51.7	0.20	0.10	0.10
C2(m2)	77.8	19.4	52.3	0.10	0.10	0.25

22/12/2009

Time (days) 7

Specimen	average depth (µm) Right bar	average depth (µm) Middle bar	average depth (µm) Left bar	crack (mm) Right bar	crack (mm) Middle bar	crack (mm) Left bar
A2(m2)	57.4	68.3	53.9	0.25	0.05	0.20
A2(m1)	55.1	67.3	58.6	0.20	0.00	0.20
B2(m)	62.8	47.4	58.0	0.25	0.00	0.20
C2(m1)	30.6	25.3	13.8	0.00	0.00	0.00
A1(m1)	72.9	68.0	63.5	0.25	0.10	0.15
B2(c)	69.6	68.3	64.3	0.20	0.10	0.00
C2(c)	53.0	43.3	65.2	0.00	0.00	0.00
A2(c)	60.3	71.3	51.1	0.23	0.00	0.15
A1(c)	60.5	62.0	76.5	0.20	0.00	0.40
A1(m2)	56.6	47.4	60.8	0.20	0.10	0.20
C2(m2)	90.3	25.1	61.2	0.15	0.10	0.25

07/01/2010

Time (days) 16

Specimen	average depth (µm) Right bar	average depth (µm) Middle bar	average depth (µm) Left bar	crack (mm) Right bar	crack (mm) Middle bar	crack (mm) Left bar
A2(m2)	77.8	96.0	74.7	0.35	0.10	0.35
A2(m1)	77.5	87.7	78.6	0.25	0.10	0.20
B2(m)	85.2	63.8	79.2	0.25	0.00	0.25
C2(m1)	53.1	35.5	24.0	0.05	0.00	0.00
A1(m1)	96.5	87.1	81.9	0.25	0.15	0.20
B2(c)	96.2	85.8	84.7	0.20	0.10	0.00
C2(c)	72.5	65.4	82.7	0.10	0.00	0.10
A2(c)	79.5	93.0	70.3	0.25	0.00	0.20
A1(c)	80.9	76.3	111.2	0.25	0.00	0.40

A1(m2)	79.1	61.7	81.6	0.20	0.10	0.20
C2(m2)	118.9	38.2	81.6	0.15	0.10	0.25

Date	14/01/2010

Specimen	Right Bar [mA]	Middle Bar [mA]	Left Bar [mA]	Total[mA]	Sum R+M+L [mA]
A2(m2)	3	5.5	4	13	12.5
A2(m1)	2	3.5	3	11	8.5
B2(m)	4	3.5	3.5	11.4	11
C2(m1)	4.2	2	2	10.5	8.2
A1(m1)	4	3.6	3	11	10.6
B2(c)	3.4	3	3.2	11	9.6
C2(c)	2.5	2	3.5	10.5	8
A2(c)	3.5	3	3.1	11	9.6
A1(c)	3.5	1	6	11	10.5
A1(m2)	4.3	2.3	3.7	10.7	10.3
C2(m2)	4.5	1	4.5	10.5	10

		average depth (µm)	average depth (µm)	average depth (µm)	crack (mm)	crack (mm)	crack (mm)
	Specimen	Right bar	Middle bar	Left bar	Right bar	Middle bar	Left bar
14/01/2010	A2(m2)	83.2	105.8	81.8	0.35	0.10	0.35
	A2(m1)	81.1	94.0	84.0	0.25	0.10	0.20
Time (days)	B2(m)	92.3	70.0	85.5	0.30	0.05	0.25
7	C2(m1)	60.6	39.0	27.5	0.05	0.00	0.00
	A1(m1)	103.7	93.6	87.2	0.25	0.15	0.20
	B2(c)	102.2	91.2	90.4	0.25	0.10	0.00
	C2(c)	77.0	68.9	89.0	0.10	0.00	0.10
	A2(c)	85.7	98.3	75.8	0.25	0.00	0.20
	A1(c)	87.1	78.1	121.9	0.25	0.00	0.40
	A1(m2)	86.8	65.8	88.2	0.20	0.10	0.20
	C2(m2)	126.9	39.9	89.7	0.15	0.10	0.25

Date	20/01/2010

Specimen	Right Bar [mA]	Middle Bar [mA]	Left Bar [mA]	Total[mA]	Sum R+M+L [mA]
A2(m2)	5.7	4.3	4.7	13	14.7
A2(m1)	3.3	5	3.7	11.7	12

		average depth (µm)	average depth (µm)	average depth (µm)	crack (mm)	crack (mm)	crack (mm)
	Specimen	Right bar	Middle bar	Left bar	Right bar	Middle bar	Left bar
20/01/2010	A2(m2)	87.5	109.1	85.4	0.40	0.12	0.35
	A2(m1)	83.6	97.8	86.8	0.27	0.10	0.22

B2(m)	3.3	3.7	3.5	12	10.5
C2(m1)	6.3	1.8	2	11.6	10.1
A1(m1)	4	4.6	2.5	12.2	11.1
B2(c)	1.5	3.6	5.8	11.4	10.9
C2(c)	4	3.3	3.8	11.7	11.1
A2(c)	3.4	3.5	3.8	11.8	10.7
A1(c)	1	3	8.9	12.3	12.9
A1(m2)	3.9	3.2	4.8	12.8	11.9
C2(m2)	5.5	2.2	3.5	12.3	11.2

Time (days)	B2(m)	94.9	72.9	88.2	0.30	0.07	0.25
6	C2(m1)	65.4	40.4	29.1	0.10	0.02	0.00
	A1(m1)	106.7	97.1	89.2	0.40	0.15	0.20
	B2(c)	103.4	93.9	94.8	0.25	0.20	0.00
	C2(c)	80.1	71.4	91.9	0.10	0.04	0.10
	A2(c)	88.3	101.0	78.7	0.30	0.00	0.25
	A1(c)	87.9	80.4	128.7	0.27	0.04	0.50
	A1(m2)	89.7	68.3	91.9	0.30	0.10	0.20
	C2(m2)	131.1	41.6	92.3	0.15	0.10	0.25

Note Starting from this date attack calculated using half of measured current,
due to current reducing progrssively over the time interval

Date	26/01/2010

Specimen	Right Bar [mA]	Middle Bar [mA]	Left Bar [mA]	Total[mA]	Sum R+M+L [mA]
A2(m2)	2.9	2.9	2.5		8.3
A2(m1)	2.5	2.9	2.6		8.0
B2(m)	2.5	2.0	2.8		7.3
C2(m1)	3.4	1.8	1.5		6.7
A1(m1)	2.7	2.6	2.1		7.4
B2(c)	2.3	2.6	3.1		8.0
C2(c)	4.5	2.2	2.3		9.0
A2(c)	2.5	2.4	2.8		7.7
A1(c)	2.4	2.5	3.8		8.7
A1(m2)	2.9	2.3	2.5		7.7
C2(m2)	2.4	2.3	3.5		8.2

		average depth (µm)	average depth (µm)	average depth (µm)	crack (mm)	crack (mm)	crack (mm)
	Specimen	Right bar	Middle bar	Left bar	Right bar	Middle bar	Left bar
26/01/2010	A2(m2)	89.7	111.3	87.3	0.40	0.12	0.40
	A2(m1)	85.6	100.0	88.8	0.30	0.10	0.24
Time (days)	B2(m)	96.8	74.4	90.3	0.40	0.10	0.35
6	C2(m1)	68.0	41.8	30.2	0.12	0.02	0.00
	A1(m1)	108.8	99.1	90.8	0.40	0.15	0.20
	B2(c)	105.1	95.9	97.2	0.30	0.20	0.00
	C2(c)	83.5	73.1	93.7	0.10	0.04	0.12
	A2(c)	90.2	102.8	80.9	0.30	0.06	0.25
	A1(c)	89.7	82.3	131.6	0.28	0.06	0.55
	A1(m2)	92.0	70.0	93.8	0.30	0.10	0.22
	C2(m2)	132.9	43.4	95.0	0.15	0.10	0.35

Date	01/02/2010

Specimen	Right Bar [mA]	Middle Bar [mA]	Left Bar [mA]	Total[mA]	Sum R+M+L [mA]
A2(m2)	1.1	2.3	2.2		5.6
A2(m1)	2.2	1.5	2.4		6.1
B2(m)	1.8	1.4	1.9		5.1
C2(m1)	2.4	1.1	1.1		4.6
A1(m1)	2.3	1.8	1.5		5.6
B2(c)	2.1	2.2	2.8		7.1
C2(c)	3.8	1.7	2		7.5
A2(c)	1.9	2	1.9		5.8
A1(c)	1.3	1.1	1		3.4
A1(m2)	1.9	2.3	2.1		6.3
C2(m2)	2.2	1.1	2.5		5.8

		average depth (μm)	average depth (μm)	average depth (μm)	crack (mm)	crack (mm)	crack (mm)
	Specimen	Right bar	Middle bar	Left bar	Right bar	Middle bar	Left bar
01/02/2010	A2(m2)	90.6	113.1	89.0	0.40	0.10	0.40
	A2(m1)	87.2	101.2	90.6	0.38	0.12	0.28
Time (days)	B2(m)	98.2	75.5	91.8	0.45	0.12	0.38
6	C2(m1)	69.8	42.6	31.1	0.15	0.02	0.00
	A1(m1)	110.6	100.5	91.9	0.45	0.16	0.20
	B2(c)	106.8	97.6	99.4	0.35	0.22	0.00
	C2(c)	86.4	74.4	95.2	0.12	0.05	0.18
	A2(c)	91.7	104.4	82.3	0.35	0.06	0.30
	A1(c)	90.7	83.1	132.4	0.28	0.06	0.55
	A1(m2)	93.4	71.8	95.4	0.33	0.10	0.30
	C2(m2)	134.6	44.2	96.9	0.20	0.10	0.38

Date	08/02/2010

Specimen	Right Bar [mA]	Middle Bar [mA]	Left Bar [mA]	Total[mA]	Sum R+M+L [mA]
A2(m2)	1.7	1.9	1.1		4.7
A2(m1)	1	1.7	1.4		4.1
B2(m)	1.5	1	1.6		4.1
C2(m1)	1.8	1.3	1.4		4.5

		average depth (μm)	average depth (μm)	average depth (μm)	crack (mm)	crack (mm)	crack (mm)
	Specimen	Right bar	Middle bar	Left bar	Right bar	Middle bar	Left bar
08/02/2010	A2(m2)	92.1	114.8	90.0	0.43	0.12	0.42
	A2(m1)	88.1	102.7	91.9	0.38	0.12	0.30
Time (days)	B2(m)	99.5	76.3	93.2	0.45	0.12	0.40
7	C2(m1)	71.4	43.8	32.3	0.15	0.02	0.00

A1(m1)	1.6	1.3	1.1		4.0
B2(c)	1.9	1.7	2.3		5.9
C2(c)	2.3	1.8	1.9		6.0
A2(c)	1.4	1.2	1.5		4.1
A1(c)	1.6	1	1.5		4.1
A1(m2)	1.8	1.4	1.7		4.9
C2(m2)	1.8	1.5	2.6		5.9

A1(m1)	112.0	101.6	92.9	0.45	0.16	0.25
B2(c)	108.4	99.1	101.4	0.37	0.22	0.00
C2(c)	88.5	76.0	96.9	0.12	0.05	0.18
A2(c)	93.0	105.4	83.7	0.35	0.06	0.30
A1(c)	92.1	84.0	133.8	0.55	0.06	0.30
A1(m2)	95.0	73.1	96.9	0.35	0.10	0.35
C2(m2)	136.2	45.6	99.3	0.20	0.10	0.38

Date 15/02/2010

Specimen	Right Bar [mA]	Middle Bar [mA]	Left Bar [mA]	Total[mA]	Sum R+M+L [mA]
A2(m2)	2.4	2.3	2.5		7.2
A2(m1)	2.5	3.4	2.6		8.5
B2(m)	2.3	1.8	2.5		6.6
C2(m1)	2.9	1.5	3		7.4
A1(m1)	4	3.5	2		9.5
B2(c)	2.8	2.4	2.9		8.1
C2(c)	2.8	2.3	2.5		7.6
A2(c)	2.5	2.3	2.7		7.5
A1(c)	7	3.5	2.8		13.3
A1(m2)	2.8	2.4	3.1		8.3
C2(m2)	2.3	2.1	2.9		7.3

15/02/2010

Time (days)

7

	average depth (µm)	average depth (µm)	average depth (µm)	crack (mm)	crack (mm)	crack (mm)
Specimen	Right bar	Middle bar	Left bar	Right bar	Middle bar	Left bar
A2(m2)	94.2	116.9	92.2	0.45	0.12	0.45
A2(m1)	90.4	105.7	94.2	0.40	0.12	0.30
B2(m)	101.5	78.0	95.4	0.45	0.15	0.40
C2(m1)	74.0	45.1	35.0	0.15	0.02	0.00
A1(m1)	115.6	104.7	94.7	0.45	0.16	0.25
B2(c)	110.9	101.3	104.0	0.37	0.22	0.00
C2(c)	91.0	78.1	99.1	0.12	0.05	0.18
A2(c)	95.2	107.5	86.1	0.35	0.10	0.30
A1(c)	98.4	87.1	136.3	0.60	0.08	0.30
A1(m2)	97.5	75.2	99.7	0.35	0.10	0.35
C2(m2)	138.3	47.4	101.8	0.40	0.10	0.25